Q3R: Quadratic Reweighted Rank Regularizer for Effective Low-Rank Training

Ipsita Ghosh*
Department of Computer Science
University of Central Florida
ipsita.ghosh@ucf.edu

Ethan Nguyen*
Department of Computer Science
University of North Carolina at Charlotte
ethan.nguyen@e-10.net

Christian Kümmerle
School of Data, Mathematical and Statistical Sciences
Department of Computer Science
University of Central Florida
kuemmerle@ucf.edu

Abstract

Parameter-efficient training, based on low-rank optimization, has become a highly successful tool for fine-tuning large deep-learning models. However, these methods fail at low-rank pre-training tasks where maintaining the low-rank structure and the objective remains a challenging task. We propose the *Quadratic Reweighted Rank Regularizer* dubbed Q3R, which leads to a novel low-rank inducing training strategy inspired by the iteratively reweighted least squares (IRLS) framework. Q3R is based on a quadratic regularizer term which majorizes a smoothed log determinant serving as rank surrogate objective. Unlike other low-rank training techniques, Q3R is able to train weight matrices with prescribed, low target ranks of models that achieve comparable predictive performance as dense models, with small computational overhead, while remaining fully compatible with existing architectures. In experiments, we are able to truncate 60% of the parameters of a ViT-Tiny parameters with marginal loss in CIFAR-10 performance and up to 80% with only 4% accuracy drop. The efficacy of Q3R is confirmed on Transformers across both image and language tasks, including for low-rank fine-tuning.

The code is available at https://github.com/ThatE10/q3r.git.

1 Introduction

Modern deep learning architectures continue to grow in size and complexity (RWC+19), creating a growing demand for efficient training methodologies. Low-rank regularization has emerged as a powerful paradigm for addressing these challenges by explicitly constraining the parameter search space through matrix factorization. This approach builds on the empirical observation that neural networks exhibit inherent low-dimensional structure in their weight matrices during training (GK+22).

Practical implementations face three key challenges: (1) performance degradation compared to full-rank baselines, (2) optimal rank selection across layers, and (3) maintaining training stability. Prior work addresses these through spectral initialization (GK+22), orthogonality regularization (YYT+20).

*Equal contribution.

39th Conference on Neural Information Processing Systems (NeurIPS 2025).

Recent advances in parameter-efficient fine-tuning (PEFT) have expanded the low-rank training paradigm through methods like Low-Rank Induced Training (LoRITa) (AZW). These approaches maintain the original model architecture during inference while inducing low-rank structure through strategic layer overparameterization during training. LoRITa specifically decomposes weight matrices $\mathbf{W}_i$ into products $\prod_{k=1}^{N} \mathbf{W}_i^k$ during optimization, enabling implicit rank reduction through singular value truncation post-training (AZW). This methodology demonstrates that explicit rank constraints can be replaced by training dynamics that naturally favor low-rank solutions.

Despite their promise, existing low-rank training approaches present several notable limitations. Traditional low-rank methods often suffer from performance degradation relative to full-rank baselines (GK$^+$22; YYT$^+$20). Methods such as LoRA and LoRITa, while effective at reducing trainable parameters, can struggle to capture the full structure making it difficult to generalize to complex tasks (AZW). Furthermore, PEFT techniques introduce additional hyperparameters (such as rank and scaling factors) whose optimal values may not generalize across architectures, datasets, or downstream tasks, often requiring extensive re-tuning and experimentation. In multilingual or low-resource settings, PEFT methods like LoRA have been observed to yield inconsistent results, sometimes improving language-specific generation at the expense of reasoning or generalization abilities (KJP$^+$25). Combining multiple PEFT modules for multi-task or continual learning can also lead to increased memory usage and system complexity, offsetting some of the intended efficiency gains. Overall, it can be observed that the advances in LoRA-type parameter-efficient training methods have not yet been able to be translated to enable robust low-rank pre-training.

2 Contribution

We propose **Quadratic Reweighted Rank Regularization** (`Q3R`), which solves the pre-existing problems by introducing an optimizer-compatible regularization framework based on smoothed log-determinant rank surrogates outlined in Section 4.1, which is specifically designed for low-rank pre-training. Our approach is theoretically grounded in saddle-escaping second-order optimization methods, and it comes with little computational overhead compared to unregularized training despite its efficacy for promoting low-rank neural network weight matrices. Additionally, we propose the Adam variant Adam`Q3R` in Section 4.2, which is tailored to optimizing `Q3R`-regularized loss functions and which improves the performance of training `Q3R`-regularized models.

Numerical experiments show that `Q3R` is able to reduce the number of parameters in ViT models by 60% during pre-training on CIFAR-10, with only around 1.3% accuracy drop. We validate the performance of `Q3R` for low-rank fine-tuning with experiments fine-tuning RoBERTa and Llama3 on GLUE tasks, for which `Q3R` achieves comparable performance compared to dense fine-tuning and state-of-the art low-rank PEFT methods. Compared to state-of-the-art low-rank training methods such as LoRA (HSW$^+$22b), LoRITa (AZW), `Q3R` consistently produces models with better generalization at high truncation levels, without requiring overparameterization or full-rank warmup phases.

In Section 4, we elaborate the methodology of the proposed work, which is further discussed with a detailed derivation in the Supplementary material in Appendix A. In Section 5, we empirically show the performance of `Q3R`, in comparison to other state-of-the-art methods. We continue with more experimental evaluations in the Supplementary material in Appendix D. Appendix D also includes discussions of the computational aspects of our methodology. In Appendix E, we demonstrate the robustness of `Q3R`to different hyperparameter variations. We briefly discuss the limitations of our work in Section 6.

3 Related Work

Parameter-Efficient Fine-Tuning (PEFT) Parameter-efficient fine-tuning is the concept of modifying only parts of a fully parametrized pre-trained model to excel at specific task of interest. PEFT methods such as adapters (HGJ$^+$19) and LoRA (HSW$^+$22b) introduce small, trainable modules into a frozen pretrained model, drastically reducing the number of parameters to be updated. These techniques often match full fine-tuning performance with only a tiny fraction of trainable parameters. However, the low-rank constraints that make LoRA-style methods efficient for downstream tasks also limit capacity if applied during pre-training. Training from scratch with only low-rank adapters or factorizations (instead of full-rank weight updates) tends to underperform, as it restricts optimization to a low-dimensional subspace (ZZC$^+$24). LoRA assumes a well-formed pretrained weight W plus a low-rank perturbation of rank-r adapter matrices $A \in \mathbb{R}^{d\times r}$ and $B \in \mathbb{R}^{r\times d}$ such that $\Delta W = AB$; without a strong initial W, such updates struggle to capture the full complexity needed for learning from scratch. *KronA* replaces LoRA's product with a Kronecker factorization for better rank-parameter trade-offs (ETK$^+$25). *DoRA* decouples update magnitude and direction via a learnable scaling factor, improving upon LoRA's expressivity (LWY$^+$24). *Compacter* uses shared, low-rank, Kronecker-parameterized adapters across layers, matching standard adapters with only 0.05 % extra parameters (MHR21).

Low-Rank Training in Neural Networks. Neural networks often exhibit implicit low-rank structure during training, as optimization dynamics like SGD with weight decay tend to bias models toward low-rank solutions (GSGP25; HMZ$^+$23). This observation has motivated a range of explicit low-rank training methods that constrain parameter matrices directly. A common approach factorizes weights and trains the factorized weights instead, reducing compute and memory costs with minor accuracy loss (KTMF21). Techniques like LoRA (WMPG24b) and its extensions (LSMR23) inject low-rank updates into pretrained Transformer weights, enabling parameter-efficient adaptation. However, pre-training directly under low-rank constraints remains more challenging. (WMPG24a) shares a similar motivation to ours—studying the limitations of LoRA-style low-rank pre-training and proposing an alternative regularization-driven approach to induce low-rank structure during training. Although we approach the problem through a different optimization framework, their analysis and framing of the limitations of adapter-based methods are highly relevant and can guide refinement of both the positioning and justification of our method. Regularization-based approaches use nuclear norm or log-determinant surrogates to promote low-rank solutions (SZCT23), while others apply orthogonality constraints and adaptive rank pruning (YYT$^+$20; YCS$^+$20). In Transformers, low-rank parameterizations have achieved 2–5$\times$ compression with minimal performance drop (AZW), and Cuttlefish (WAUc$^+$23) automates rank selection by monitoring stable ranks during a warmup phase. Still, many methods rely on post-hoc truncation or overparameterization, which do not minimize rank during training. Our work addresses this gap by directly optimizing for low-rank solutions via reweighted least squares, promoting compact representations throughout pre-training. However, many of these methods rely on overparameterization or post-hoc truncation and do not directly minimize rank during training. In contrast, our approach promotes low-rank structure directly via optimization, using a principled regularization technique rooted in reweighted least squares.

Spectral Low-Rank Regularization. A related line of work studies algorithms that impose low-rankness of neural network matrices based on the nuclear norm, Schatten-p quasi-norm or a direct rank regularization. In particular, (AS17) proposed a proximal stochastic gradient descent applied to the nuclear norm. Methods that apply spectral truncation (e.g., via truncated SVD) during training or post-training (YTW$^+$20; XLZ$^+$20) can also be understood within this framework. A downside of such approaches is the computational overhead: they require at least a truncated SVD at *every* iteration, which quickly becomes computationally prohibitive for larger networks. Moreover, arguably, such aggressive, discontinuous rank regularization interferes with the continuous gradient-based training process of the network.

In contrast, our proposed `Q3R` regularizer imposes low-rankness more *gradually* by reweighting at periodic intervals, at which a smoothing parameter is updated as well, which we find to be sufficient for convergence while significantly reducing the computational overhead. This "soft" imposition of low-rank structure aligns with insights from IRLS-based methods (see below). A spectral, Schatten-p regularization is also the core of the motivation of LoRITa (AZW); however, in this case, the spectral regularization can be seen as a justification of an (unweighted) squared Frobenius norm regularization on factor matrices, whereas `Q3R` does not work with factor matrices and considers a *reweighted* quadratic term.

Rank Regularization and IRLS. In a line of work that significantly precedes the interest in low-rank techniques for deep learning, the problem of identifying or learning a low-rank matrix from noisy, under-determined linear measurements has been studied for decades in control theory (FHB03; DCM22), recommender systems (Kor09; KBV09) and compressed sensing (RFP10; DR16). Even in this setting, which is fundamentally linear unlike the training of deep neural networks, the minimization of a rank objective subject to the constraints is NP-hard (Nat95; RFP10) , motivating surrogate formulations or relaxations. Convex relaxations using the nuclear norm (CR09; RFP10;

DR16; CW18) have been popular for a long time due to their strong recovery guarantees under suitable assumptions and their ability to be tackled using the machinery of convex optimization (BV04), but fail to result in a convex formulation in the deep learning setting. Even disregarding computational limitations of convex regularizations (CC18), *non-convex* rank surrogates such as the log-determinant penalty (FHB03) lead to algorithms which are more data-efficient as a evidenced for a variety of low-rank matrix recovery problems (FHB04; CESV13; KS18; KM23).
If combined with a suitable smoothing strategy, the non-smooth optimization framework of Iteratively Reweighted Least Squares (IRLS), originally pioneered by Weiszfeld (Wei37; WP09; BS15), has emerged as a leading algorithmic framework to optimize non-convex rank surrogates (FRW11; MF10; KMV21; GTK24) as it provides good trade-offs between scalability, data-efficiency, saddle-point evasion (present due to inherent non-convexity) and fast convergence. On a high level, IRLS solves a sequence of weighted Frobenius-norm problems that progressively suppress smaller singular values. The proposed rank regularization term `Q3R` (detailed in Section 4.1) builds on recent improvements on low-rank IRLS weight operator formulations (KMV21; GTK24) (or reweighting strategies), which, unlike older formulations (FRW11; MF10), allow for fast saddle-point evasion and locally quadratic convergence rates. To the best of our knowledge, IRLS-type low-rank regularization, which is at the core of `Q3R`, has not been explored in the literature in the context of deep learning so far. While providing an interesting perspective on older IRLS formulations (FRW11; MF10) from an *average gradient outer product* perspective, the recent work (RBD25) does not provide insights towards the derivation of quadratically convergent IRLS methods (KMV21; GTK24), nor does it extend the framework towards low-rank training of deep networks.

In the language of the low-rank recovery literature, LoRA-type (HSW$^+$22a) approaches are known under the name of (*Burer-Monteiro* (BM03)) matrix factorization methods (SL16; ZL15; MWCC20; CLC19; ZCZ22; XSCM23; SZ25). While popular in applications (KBV09; RKZK22) due to their scalability, it is known that they can be outperformed by IRLS or Riemannian optimization approaches in more challenging setups involving, e.g., limited data (ZN22; LHLZ24), which is one motivation of our work.

4 Methodology

In this section, we provide a detailed derivation and definition of the *Quadratic Reweighted Rank Regularizer* `Q3R` in Section 4.1, before we embed it into a training scheme to train low-rank weights of deep learning models in Section 4.2.

4.1 Low-Rank Regularization via `Q3R`

Given a neural network with K weight matrices $\Theta = \{\mathbf{W}_i : \mathbf{W}_i \text{ is weight matrix}, i = 1, \ldots, K\}$, a functionally ideal regularization term to add to the loss function of the network for the promotion of a low-rank weight is simply the *rank* of $\mathbf{W}$. However, $\operatorname{rank}(\mathbf{W})$ is non-convex and not continuous, and thus hard to incorporate into a gradient-based training methodology.

In the following, we consider the *non-convex*, but continuously differentiable rank surrogate $F_\epsilon(\cdot)$ called ϵ-*smoothed log-determinant*, defined as

$$F_\epsilon(\mathbf{W}) := \sum_{i=1}^{d} f_\epsilon(\sigma_i(\mathbf{W})), \text{ where } f_\epsilon(\sigma) = \begin{cases} \epsilon^2 \left(\log(\sigma) - \log(\epsilon)\right) + \frac{1}{2}\epsilon^2, & \text{if } \sigma \geqslant \epsilon, \\ \frac{1}{2}\sigma^2, & \text{if } \sigma < \epsilon, \end{cases} \tag{1}$$

where $\sigma_i(\mathbf{W})$ is the i-th singular value of $\mathbf{W}$, and which is parametrized by a smoothing parameter $\epsilon > 0$. The definition of (1) follows (KM23) and is related to the log-determinant heuristics $\log\det(\mathbf{W} + \epsilon I) = \sum_{i=1}^{d} \log(\sigma_i(\mathbf{W}) + \epsilon)$ defined for positive semi-definite matrices $\mathbf{W} \in \mathbb{R}^{d\times d}$ of (FHB03; CESV13; RBD25). Compared to other log-determinant type functions, $F_\epsilon(\cdot)$ from (1) has a few advantages: It is lower bounded by 0 for any ϵ and has a 1-Lipschitz gradient, making the objective compatible with gradient-based optimizers without extensive step-size adaptation. Furthermore, its smoothing parameter ϵ *regulates* the non-convexity of its optimization landscape and recovers the well-known squared Frobenius norm as $F_\epsilon(\mathbf{W}) = \frac{1}{2}\|\mathbf{W}\|_F^2$ in the case of $\sigma_1(\mathbf{W}) < \epsilon$.

The rank regularizer we study in this paper, however, is not simply $F_\epsilon(\cdot)$: If we were to work directly with the ϵ-smoothed log-determinant, its gradients $\nabla F_\epsilon(\mathbf{W})$ would require a full spectral decomposition of $\mathbf{W}$ at each training iteration (see supplementary material).

Instead, we consider, given an expansion center point $\mathbf{W}'$ (which may correspond to the current weight matrix during a neural network training dynamics), the *quadratic model* $Q_\epsilon(\cdot|\mathbf{W}')$ defined as

$$Q_\epsilon(\mathbf{W} \mid \mathbf{W}') = F_\epsilon(\mathbf{W}') + \tfrac{1}{2}\langle \mathbf{W}, \mathcal{R}_{\mathbf{W}',\epsilon}(\mathbf{W})\rangle - \tfrac{1}{2}\langle \mathbf{W}', \mathcal{R}_{\mathbf{W}',\epsilon}(\mathbf{W}')\rangle, \tag{2}$$

where $\mathcal{R}_{\mathbf{W}',\epsilon}(\cdot) : \mathbb{R}^{d_1\times d_2} \to \mathbb{R}^{d_1\times d_2}$ is a positive definite, so-called *reweighting operator* (KMV21; GTK24), defined in Definition 4.1 below.

Definition 4.1 (Reweighting Operator (KM23))**.** *Let $\epsilon > 0$ and $\mathbf{W}' \in \mathbb{R}^{d_1\times d_2}$ be a matrix with singular value decomposition $\mathbf{W}' = \mathbf{U}_{\mathbf{W}'}\operatorname{diag}(\sigma_i(\mathbf{W}'))\mathbf{V}_{\mathbf{W}'}^\top$, where $\mathbf{U} \in \mathbb{R}^{d_1\times r(\mathbf{W}',\epsilon)}$ and $\mathbf{V} \in \mathbb{R}^{d_2\times r(\mathbf{W}',\epsilon)}$ are matrices of the leading $r(\mathbf{W}',\epsilon)$ left and right singular vectors satisfying $\mathbf{U}_{\mathbf{W}'} = [\mathbf{U} \quad \mathbf{U}_\perp] \in \mathbb{R}^{d_1\times d_1}$ and $\mathbf{V}_{\mathbf{W}'} = [\mathbf{V} \quad \mathbf{V}_\perp] \in \mathbb{R}^{d_2\times d_2}$, and*

$$r(\mathbf{W}',\epsilon) := |\{i \in \{1,\ldots,\min(d_1,d_2)\} : \sigma_i(\mathbf{W}') > \epsilon\}| \tag{3}$$

is the number of singular values of $\mathbf{W}'$ larger than ϵ. Then we define the reweighting operator *$\mathcal{R}_{\mathbf{W}',\epsilon} : \mathbb{R}^{d_1\times d_2} \to \mathbb{R}^{d_1\times d_2}$ associated to the matrix $\mathbf{W}'$ and smoothing parameter ϵ as*

$$\mathcal{R}_{\mathbf{W}',\epsilon}(\mathbf{W}) = \mathbf{U}_{\mathbf{W}'}\Sigma_{\epsilon,d_1}^{-1}\mathbf{U}_{\mathbf{W}'}^\top\mathbf{W}\mathbf{V}_{\mathbf{W}'}\Sigma_{\epsilon,d_2}^{-1}\mathbf{V}_{\mathbf{W}'}^\top,$$

where $\Sigma_{\epsilon,d} = \operatorname{diag}(\max(\sigma_i(\mathbf{W}')/\epsilon, 1))_{i=1}^d \in \mathbb{R}^{d\times d}$ for $d \in \{d_1, d_2\}$.

The reweighting operator satisfies the following simple properties (shown in the supplementary material), which makes working with it computationally feasible.

Lemma 4.1. *For $\epsilon > 0$ and $\mathbf{W}'$, let $\mathbf{U} \in \mathbb{R}^{d_1\times r(\mathbf{W}',\epsilon)}$, $\mathbf{V} \in \mathbb{R}^{d_1\times r(\mathbf{W}',\epsilon)}$ and $\mathcal{R}_{\mathbf{W}',\epsilon} : \mathbb{R}^{d_1\times d_2} \to \mathbb{R}^{d_1\times d_2}$ be as in Definition 4.1. Then the following statements are true:*

1. $\mathcal{R}_{\mathbf{W}',\epsilon}(\cdot)$ is a positive definite operator with respect to the Frobenius inner product $\langle \mathbf{A}, \mathbf{B}\rangle = \operatorname{tr}(\mathbf{A}^\top\mathbf{B})$, i.e., $\langle \mathbf{W}, \mathcal{R}_{\mathbf{W}',\epsilon}(\mathbf{W})\rangle > 0$ for all non-zero $\mathbf{W} \in \mathbb{R}^{d_1\times d_2}$.

2. The image $\mathcal{R}_{\mathbf{W}',\epsilon}(\mathbf{W})$ of any $\mathbf{W} \in \mathbb{R}^{d_1\times d_2}$ w.r.t. the reweighting operator can be computed as

$$\begin{aligned}\mathcal{R}_{\mathbf{W}',\epsilon}(\mathbf{W}) &= \epsilon^2\mathbf{U}\Sigma^{-1}\mathbf{U}^\top\mathbf{W}\mathbf{V}\Sigma^{-1}\mathbf{V}^\top + \epsilon\mathbf{U}\Sigma^{-1}\mathbf{U}^\top\mathbf{W}(\mathbf{I} - \mathbf{V}\mathbf{V}^\top) \\ &\quad + \epsilon(\mathbf{I} - \mathbf{U}\mathbf{U}^\top)\mathbf{W}\mathbf{V}\Sigma^{-1}\mathbf{V}^\top + (\mathbf{I} - \mathbf{U}\mathbf{U}^\top)\mathbf{W}(\mathbf{I} - \mathbf{V}\mathbf{V}^\top),\end{aligned} \tag{4}$$

where $\Sigma = \operatorname{diag}(\sigma_i(\mathbf{W}'))_{i=1}^{r(\mathbf{W}',\epsilon)} \in \mathbb{R}^{r(\mathbf{W}',\epsilon)\times r(\mathbf{W}',\epsilon)}$ is the diagonal matrix containing the largest $r(\mathbf{W}',\epsilon)$ singular values of $\mathbf{W}'$.
3. The quadratic model of (2) satisfies, for all $\mathbf{W}, \mathbf{W}' \in \mathbb{R}^{d_1\times d_2}$, that

$$Q_\epsilon(\mathbf{W} \mid \mathbf{W}') = F_\epsilon(\mathbf{W}') + \langle \nabla F_\epsilon(\mathbf{W}'), \mathbf{W} - \mathbf{W}'\rangle + \tfrac{1}{2}\langle \mathbf{W} - \mathbf{W}', \mathcal{R}_{\mathbf{W}',\epsilon}(\mathbf{W} - \mathbf{W}')\rangle. \tag{5}$$

We note that the quadratic model $Q_\epsilon(\cdot \mid \mathbf{W}')$ (2) defined by $\mathcal{R}_{\mathbf{W}',\epsilon}$ is a *majorizing* quadratic model that satisfies $Q_\epsilon(\mathbf{W}|\mathbf{W}') \geqslant F_\epsilon(\mathbf{W})$ for all $\mathbf{W} \in \mathbb{R}^{d_1\times d_2}$.[2] It is *different* from a second-order Taylor expansion of the $F_\epsilon(\cdot)$ about $\mathbf{W}'$, which would only be an *approximation, but no majorization* due to the non-convex nature of $F_\epsilon(\cdot)$. The quadratic model can still be related to a second-order Taylor expansion of F_ϵ via (5) as each generalized Hessian (HUSN84) $\partial^2 F_\epsilon(\mathbf{W}')$ of F_ϵ satisfies $\partial^2 F_\epsilon(\mathbf{W}') \preceq \mathcal{R}_{\mathbf{W}',\epsilon}$ in the Loewner order.

We observe that in the quadratic model $Q_\epsilon(\mathbf{W} \mid \mathbf{W}')$ of (2), the only term that depends on $\mathbf{W}$ is the second summand. Thus, to obtain a simple, *differentiable* regularizer term that can be incorporated into a deep learning framework, we define the *Quadratic Reweighted Rank Regularizer* `Q3R` of a neural network weight matrix $\mathbf{W} \in \mathbb{R}^{d_1\times d_2}$, given $\mathbf{W}' \in \mathbb{R}^{d_1\times d_2}$ and $\epsilon > 0$, as $\mathrm{Q3R}_{\mathbf{W}',\epsilon} : \mathbb{R}^{d_1\times d_2} \to \mathbb{R}$ with

$$\mathrm{Q3R}_{\mathbf{W}',\epsilon}(\mathbf{W}) = \frac{1}{2}\langle \mathbf{W}, \mathcal{R}_{\mathbf{W}',\epsilon}(\mathbf{W})\rangle. \tag{6}$$

As we see in the next section, it is simple and tractable to compute its gradient $\nabla_{\mathbf{W}}\,\mathrm{Q3R}_{\mathbf{W}',\epsilon}(\mathbf{W}) \in \mathbb{R}^{d_1\times d_2}$, which can be used by any gradient-based optimizer.

[2] This majorization property is implicitly postulated in (KMV21; KM23), but without proof. While proving this property is beyond the scope of this paper, we believe that the statement is true.

Algorithm 1 Update Reweighting Operator $\mathcal{R}_{\mathbf{W}',\epsilon_{\text{old}}}(\cdot) \mapsto \mathcal{R}_{\mathbf{W},\epsilon_{\text{new}}}(\cdot)$

Input: NN weight matrix $\mathbf{W} \in \mathbb{R}^{d_1 \times d_2}$; target rank r_{target}; prev. smoothing parameter ϵ_{old}.
Output: Updated ϵ_{new}, reweighting operator $\mathcal{R}_{\mathbf{W},\epsilon_{\text{new}}}$ (via Σ, $\mathbf{U}$, $\mathbf{V}$), envelope rank r_{env}
Compute $[\mathbf{U}, \Sigma, \mathbf{V}] = \text{SVD}^{\epsilon_{\text{old}}}(\mathbf{W})$ of $\mathbf{W}$, where $\text{SVD}^{\epsilon_{\text{old}}}(\cdot)$ computes a partial singular value decomposition of its input up to order $r(\cdot, \epsilon_{\text{old}})$ (see (3)) as well as $\sigma_{r_{\text{target}}+1}(\mathbf{W})$.
$\epsilon_{\text{new}} = \min\big(\epsilon_{\text{old}}, \sigma_{r_{\text{target}}+1}(\mathbf{W})\big)$. ▷ UPDATE SMOOTHING (7)
$r_{\text{env}} = r(\mathbf{W}, \epsilon_{\text{new}})$ ▷ UPDATE RANK ENVELOPE
Set $\mathbf{U} = \mathbf{U}_{:,1:r_{\text{env}}}$, $\mathbf{V} = \mathbf{V}_{:,1:r_{\text{env}}}$, $\Sigma = \Sigma_{1:r_{\text{env}},1:r_{\text{env}}}$ ▷ RESTRICT PART. SVD MATRICES
return Reweighting operator $\mathcal{R}_{\mathbf{W},\epsilon_{\text{new}}}$ implicitly defined by $\mathbf{U} \in \mathbb{R}^{d_1 \times r_{\text{env}}}$, $\mathbf{V} \in \mathbb{R}^{d_2 \times r_{\text{env}}}$, Σ & ϵ_{new}.

Furthermore, we periodically (but not at each training iteration) *update* the reweighting operator of `Q3R` (and thus, the underlying quadratic model $Q_\epsilon(\mathbf{W} \mid \mathbf{W}')$) by setting $\mathbf{W}' \leftarrow \mathbf{W}$ and re-compute $\mathcal{R}_{\mathbf{W}',\epsilon}$, for which a truncated SVD of $\mathbf{W}$ is sufficient due to (4). Additionally, whenever updating $\mathcal{R}_{\mathbf{W}',\epsilon}$, we apply the *non-increasing* update

$$\epsilon \leftarrow \min(\epsilon, \sigma_{r_{\text{target}}+1}(\mathbf{W})) \tag{7}$$

to the smoothing parameter ϵ, which uses a *target rank* parameter r_{target} as an input. The rationale of this smoothing parameter update is two-fold: first, this choice gives *partial control* on the expected rank of the weight matrix after training, as the value of $\mathcal{R}_{\mathbf{W}',\epsilon}(\mathbf{W})$ tends to 0 if ϵ follows the dynamics of (7) in the case of $\epsilon \to 0$ for matrices $\mathbf{W}$ whose row and column spaces are both orthogonal to the columns of $\mathbf{U}$ and $\mathbf{V}$, respectively. Second, this choice increases the *non-convexity* the ϵ-smoothed log-determinant F_ϵ underlying `Q3R` *gradually* (YATC20), facilitating a fast convergence to true low-rank solutions without becoming trapped in high-rank local minima (KMV21; KM23). We summarize computational steps of a reweighting operator update in Algorithm 1.

4.2 Neural Network Training via AdamQ3R

Let now $y : \mathbb{R}^{d_1^1 \times d_2^1} \times \mathbb{R}^{d_1^K \times d_2^K} \times \mathbb{R}^{d_{\text{in}}} \to \mathbb{R}^{d_{\text{out}}}$ be the input-output mapping of a deep neural network that depends on weight parameter matrices $\Theta = \{\mathbf{W}_k \in \mathbb{R}^{d_1^k \times d_2^k} : \mathbf{W}_k \text{ is weight matrix}, k = 1, \ldots, K\}$. For a Transformer-based architecture such as Vision Transformer (DBKea21), the weight matrices include square layer- and head-wise query, key and value weight matrices $\mathbf{W}_q, \mathbf{W}_k, \mathbf{W}_v \in \mathbb{R}^{d \times d}$ as well as rectangular projection and MLP layer weight matrices. Given a pairwise loss $\ell(\cdot,\cdot)$ such as cross entropy and a training dataset $\{x_i, y_i\}_{i=1}^n$, we can define the (unregularized) network loss as $\mathcal{L}(\Theta) = \frac{1}{n}\sum_{i=1}^n \ell\big(y(\Theta, x_i), y_i\big)$.

In order to gradually impose low-rank weights during training, we propose to optimize instead the `Q3R`-regularized total loss $\mathcal{L}_{\texttt{Q3R}}(\Theta) := \mathcal{L}(\Theta) + \lambda \sum_{k=1:\texttt{Q3R}\text{ is active for }\mathbf{W}_k}^K \text{Q3R}_{\mathbf{W}'_k,\epsilon_k}(\mathbf{W}_k)$, where $\lambda > 0$ is a regularization parameter and the $\text{Q3R}_{\mathbf{W}'_k,\epsilon_k}(\cdot)$ are as in (6); the $\{\mathbf{W}'_k\}$ are initially set to the initialization weights, and $\epsilon_k = \infty$ for each $k = 1, \ldots, K$. We observe that due to the definition of `Q3R`, the gradient with respect to the regularizer terms can be computed as $\nabla_{\mathbf{W}_k} \text{Q3R}_{\mathbf{W}'_k,\epsilon_k}(\mathbf{W}_k) = \mathcal{R}_{\mathbf{W}'_k,\epsilon_k}(\mathbf{W}_k)$ for each k, i.e., by computing the image of $\mathbf{W}_k$ with respect to the reweighting operator $\mathcal{R}_{\mathbf{W}'_k,\epsilon_k}(\cdot)$ of Definition 4.1.

Algorithm 2 Low-Rank Training via Adam`Q3R`

Input: Minibatch size B, reweighting period T, `Q3R` parameter λ, learning rate $\alpha = 0.001$, $\beta_1 = 0.9$, $\beta_2 = 0.999$, $\delta = 10^{-8}$, $\eta = 3$, target rank r_{target}.
Initialize parameter $\mathbf{W}_0$, ϵ_0 and reweighting operator $\mathcal{R}_{\mathbf{W}_0,\epsilon_0}$
for $t = 0, 1, \ldots$ **do**
  if $t \bmod T = 0$ **then**
    Update reweighting operator $\mathcal{R}_{\lfloor \frac{t}{T} \rfloor}(\cdot) := \mathcal{R}_{\mathbf{W}_t,\epsilon_t}(\cdot)$ and ϵ_t ▷ USE ALGORITHM 1
  end if
  Sample minibatch $S = \{(x_i, y_i)\}_{i=1}^B$
  $\mathbf{g}_{t+1} \leftarrow \nabla_{\mathbf{W}} \mathcal{L}_S(\mathbf{W}_t)$ ▷ COMPUTE BATCH GRADIENT OF $\mathcal{L}$
  $\mathbf{m}_{t+1} \leftarrow \beta_1 \mathbf{m}_t + (1-\beta_1)\mathbf{g}_{t+1}$
  $\mathbf{v}_{t+1} \leftarrow \beta_2 \mathbf{v}_t + (1-\beta_2)\mathbf{g}_{t+1}^2$
  $\hat{\mathbf{m}}_{t+1} \leftarrow \mathbf{m}_{t+1}/(1-\beta_1^{t+1})$
  $\hat{\mathbf{v}}_{t+1} \leftarrow \mathbf{v}_{t+1}/(1-\beta_2^{t+1})$
  $\mathbf{R}_t \leftarrow \mathcal{R}_{\lfloor \frac{t}{T} \rfloor}(\mathbf{W}_t)$ ▷ COMPUTE `Q3R` GRADIENT (4)
  $\mathbf{W}_{t+1} \leftarrow \mathbf{W}_t - \eta\Big(\frac{\alpha \hat{\mathbf{m}}_{t+1}}{\sqrt{\hat{\mathbf{v}}_{t+1}} + \delta} + \lambda \mathbf{R}_t\Big)$
end for
return $\mathbf{W}_t$

The `Q3R`-regularized loss $\mathcal{L}_{\texttt{Q3R}}$ can now be used in conjunction with any optimizer suitable for the neural network architecture such as minibatch stochastic gradient or Adam (A$^+$14). To ensure that the quadratic models underlying `Q3R` match the ϵ_k-smoothed log-determinant rank surrogates

F_{ϵ_k} (1) closely, we update the reweighting operators $\mathcal{R}_{\mathbf{W}'_k,\epsilon_k}(\cdot)$ via Algorithm 1 on a fixed iteration schedule of every T training iterations–we call this parameter T the *reweighting period*.

However, instead of using a generic adaptive gradient optimizer such as Adam on $\mathcal{L}_{\texttt{Q3R}}$, we observe that the Q3R terms already possess accurate second-order information of underlying regularization surrogate, which means that including the Q3R terms into the adaptive part of an Adam-like optimizer is likely to be suboptimal. For this reason, we propose to use a dedicated adaptive optimizer to optimize $\mathcal{L}_{\texttt{Q3R}}$, dubbed *AdamQ3R*, which is detailed in Algorithm 2. AdamQ3R extends the observation of AdamW (LH19) that a decoupling of regularization term (in that case, squared Frobenius norm regularization) and network loss improves generalization performance to Q3R regularization, avoiding a distortion of the loss landscape. A validation of the benefits of using AdamQ3R vs. standard Adam applied to $\mathcal{L}_{\texttt{Q3R}}$ can be found in the supplementary material.

Computational Aspects. Following the low-rank training framework of Q3R, for example, via AdamQ3R, introduces a limited computational overhead compared to unregularized deep learning. Every T training iterations, a truncated singular value decomposition of order r_{env} (see Algorithm 1) of each weight matrix $\mathbf{W}_i \in \mathbb{R}^{d_1 \times d_2}$ to which Q3R is applied is required, which has a time complexity of $O(d_1 d_2 r_{\text{env}} + (d_1 + d_2) r_{\text{env}}^2)$ (HMT11). Similarly, calculating a Q3R gradient $\mathbf{R}_t$ in Algorithm 2 imposes a total cost of $O\big(d_1 d_2 r_{\text{env}} + (d_1 + d_2) r_{\text{env}}^2 + r_{\text{env}}^3\big)$. Since the smoothing parameter update rule (7) is designed to relate r_{env} with the target rank r_{target} such that $r_{\text{env}} \approx r_{\text{target}}$, the additional time complexity is somewhat proportional to the target rank. To obtain significant parameter reductions in the trained network weight matrices, it is chosen such that $r_{\text{target}} \ll \min(d_1, d_2)$, which limits the computational overhead of Q3R in the most interesting use cases. Additional memory requirements amount to $r_{\text{env}}(d_1 + d_2 + 1)$ per weight matrix as the reweighting operator information needs to be stored via $\mathbf{U}, \mathbf{V}$ and Σ.

5 Experiments

We explore the ability of Q3R to obtain favorable trade-offs between model performance and parameter-efficiency across diverse architectures and data distributions experimentally. To this end, we compare different low-rank training methodologies across a range of architecture-dataset pairs: we pre-train ViT-Tiny (DBKea21; SKZ+22) on CIFAR-10, ViT-Base (DBKea21) on CIFAR-100, followed by post-training low-rank truncation (AZW); further, we fine-tune BERT-Large (DCLT19) on GLUE benchmark tasks (without truncation).

5.1 Low-Rank Pre-Training

We compare the accuracy of models trained by Q3R against baselines LoRITa (AZW), LoRA (HSW+22a), and a model trained without low-rank regularization, after post-training truncation. After training, we truncate each layer weight matrix $\mathbf{W}_k \in \Theta$ using a truncated SVD to obtain factor matrices $\mathbf{A}, \mathbf{B}$ with inner dimension r and $\mathbf{W}_k \approx \mathbf{AB}$ for a range of ranks r corresponding to different parameter retention percentages p. Depending on the experiment, we apply low-rank regularization to different subsets of weights $\{\mathbf{W}_k\}$.

ViT-Tiny Trained on CIFAR-10. We train ViT-Tiny on CIFAR-10 for 100 epochs using a learning rate of $\alpha = 0.00004$. We enable low-rank training for all Transformer blocks, accounting for 96% of ViT-Tiny's parameters. We conduct a hyperparameter sweep across different configurations, and Figure 1a shows the best performance achieved by each training method when rank regularization is applied to the MLP and QKV weights. From Table 1, we find that AdamQ3R retains 42.4% of the original parameters with only a 1.22% performance drop, and retains 23.2% of parameters with a 4.4% performance drop, while LoRITa consistently underperforms in comparison. As shown in Figure 1b, despite various hyperparameter configurations λ and d for LoRITa, AdamQ3R consistently outperforms LoRITa upon truncation.

ViT-Base Trained on CIFAR-100. To demonstrate the performance of the low-rank pre-training methods on a more challenging dataset and larger model, we train the $86M$ parameter ViT-Base from scratch for 100 epochs on CIFAR-100 with data augmentation and $\alpha = 0.0001$ (SKZ+22). In line with practice for large-scale Transformers (LFX+24), we apply low-rank training techniques solely to

Model\Parameter Retetion p	**5%**	**10%**	**15%**	**20%**	**30%**	**40%**	**100%**
Vanilla ViT-T	0.1475	0.1252	0.1350	0.1213	0.1624	0.1524	0.6840
LoRA	-	0.3546	0.3655	0.3576	-	-	-
LoRITa D=2, λ=10^{-1}	0.0989	0.1433	0.1543	0.2125	0.3247	0.4523	0.7142
LoRITa D=3, λ=10^{-1}	0.2258	0.3861	0.4466	0.5035	0.6368	0.6740	0.7273
LoRITa D=3, λ=10^{-3}	0.1338	0.2136	0.3839	0.4560	0.5973	0.6253	**0.7449**
Q3R, $r_{\text{target}} = 10\%$, λ=10^{-3}	**0.2322**	0.4085	0.5606	0.6295	0.6526	0.6654	0.6843
Q3R, $r_{\text{target}} = 15\%$, λ=10^{-3}	0.1796	**0.4758**	0.5883	0.6215	0.6455	0.6555	0.6737
Q3R, $r_{\text{target}} = 20\%$, λ=10^{-3}	0.1998	0.4737	**0.6175**	0.6511	**0.6749**	**0.6833**	0.6990
Q3R, $r_{\text{target}} = 10\%$, λ=10^{-2}	0.2041	0.4387	0.6115	0.6449	0.6707	0.6771	0.6889
Q3R, $r_{\text{target}} = 15\%$, λ=10^{-2}	0.1313	0.3896	0.6158	**0.6550**	0.6689	0.6801	0.6982
Q3R, $r_{\text{target}} = 20\%$, λ=10^{-2}	0.1870	0.4335	0.6123	0.6496	0.6744	0.6868	0.6962

Table 1: MLP truncation performance of ViT-T, rank regularization is applied to *both* attention (QKV) blocks and MLP blocks. For LoRA, factor ranks are adaptive to p.

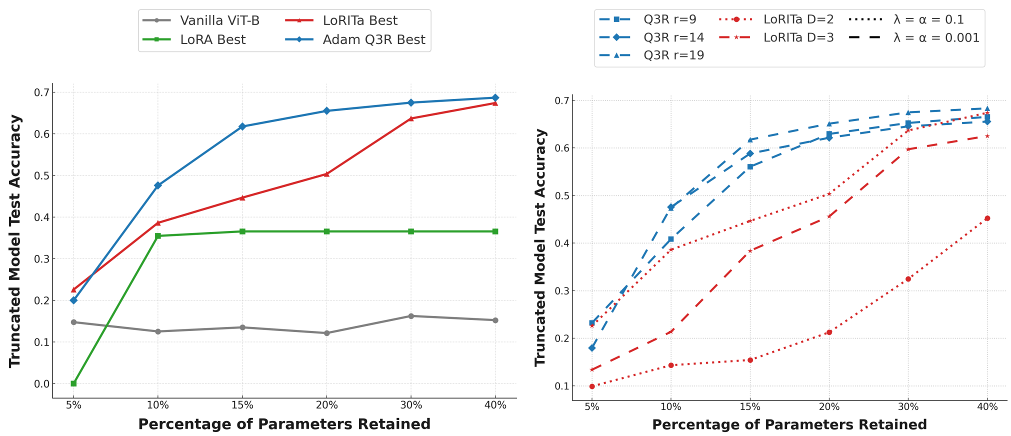

(a) Upper Bounds Comparison

(b) AdamQ3R vs. LoRITa Variants

Figure 1: Performance curves on CIFAR-10 with rank regularization applied to MLP and QKV blocks: (a) Best performance across methods, (b) AdamQ3R vs. LoRITa variants.

the multi-head self attention blocks (QKV, but not to the MLP blocks). Despite the additional size and complexity of ViT-Base compared to ViT-Tiny, `Q3R` remains robust and exhibits larger performance advantages with 0.40-0.44 test accuracy at 20% parameters retained, whereas LoRITa models do not exceed an accuracy of 0.25 at the same truncation level despite their substantial overparametrization (Figures 2a and 2b).

ViT-Tiny with Low-Rank Attention Weights. We train ViT-Tiny for 100 epochs on CIFAR-10 (Kri09) from scratch with learning rate $\alpha = 0.0004$, with low-rank regularization applied only to attention weights. We evaluate the methods for a larger set of hyperparameters as shown in Figure 3b using layer-wise truncation levels with retained parameter percentages $p \in \{5\%, 10\%, 15\%, 20\%, 30\%, 40\%, 50\%, 60\%, 70\%, 80\%, 90\%\}$, and present results in Figure 3. Figure 3a shows that `Q3R` experiences almost no performance drop up to $p = 30\%$ for most parameter choices, exceeding the performance of reference methods. Figure 3b shows that the worst performing `Q3R` model still outperforms any LoRA, LoRITa, or vanilla ViT-Tiny below $p = 60\%$, showcasing the method's robustness.

ViT-Base on ImageNet-1k. We train ViT-Base on ImageNet-1k using Automatic Mixed Precision (MNA[+]18) with AutoAugmentation (CZM[+]19) for 100 epochs. Training is conducted with a learning rate of $\alpha = 4 \times 10^{-5}$, a batch size of 384, and gradient clipping (ZHSJ20) across 4 L40S GPUs. We observe that `Q3R` consistently outperforms the baseline model while utilizing fewer

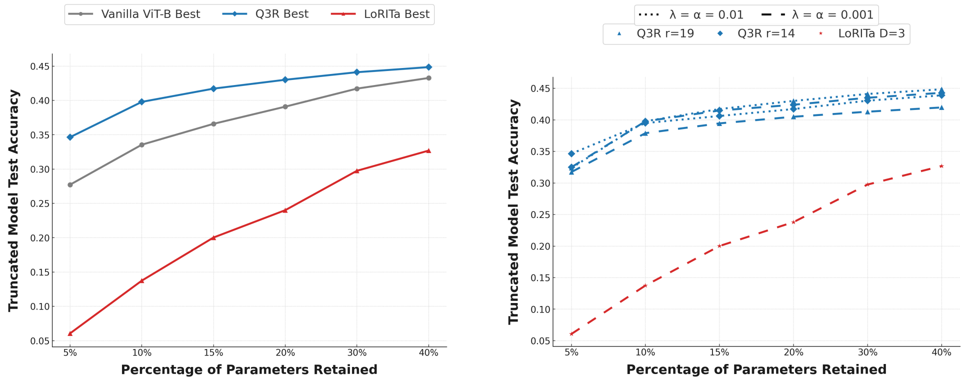

(a) Upper Bounds Comparison

(b) AdamQ3R vs. LoRITa Variants

Figure 2: Performance curves on CIFAR-100 with rank regularization applied to QKV blocks: (a) Best performance across methods, (b) AdamQ3R vs. LoRITa variants.

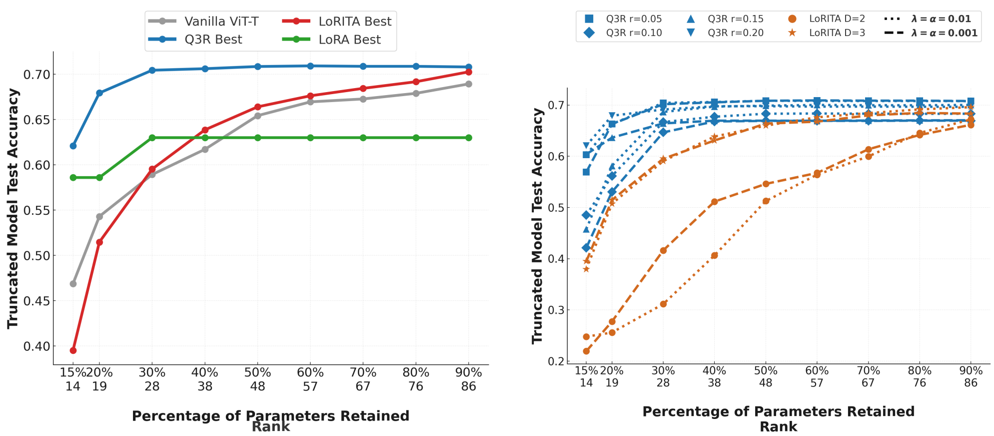

(a) Upper Bounds Comparison

(b) AdamQ3R vs. LoRITa Variants

Figure 3: Performance curves on CIFAR-10 with rank regularization applied to QKV blocks: (a) Best performance across methods, (b) AdamQ3R vs. LoRITa variants.

parameters. This performance advantage holds under two truncation paradigms: attention matrices only, and entire Transformer blocks. In both cases, `Q3R` maintains performance comparable to the full baseline model, as seen in Table 2.

Optimizer | Transformer Modules	0.1	0.15	0.2	0.3	0.4	0.5	1
AdamQ3R | QKV, MLP	0.0138	**0.1439**	**0.3376**	**0.421**	**0.4458**	**0.4556**	**0.5816**
Adam | QKV, MLP	**0.0193**	0.0976	0.2950	0.399	0.4311	0.4523	0.5179
AdamQ3R | QKV	0.1713	0.3016	**0.4623**	**0.4895**	**0.4952**	**0.4975**	**0.5816**
Adam | QKV	**0.2552**	**0.3366**	0.4551	0.4882	0.4882	0.4937	0.5179

Table 2: ViT-Base on ImageNet-1k validation accuracy post-truncation on the last epoch

5.2 Low-Rank Fine-Tuning

`Q3R` not only induces a low-rank structure during pre-training in a memory-efficient manner, but also extends naturally to compact fine-tuning. We fine-tune pre-trained RoBERTa models on the GLUE benchmark using AdamQ3R with the proposed `Q3R` regularizer, and compare against full fine-tuning and LoRA (HSW$^+$22b). We impose `Q3R` on the weight matrices that are added to the full-rank pretrained weight matrices. For LoRA, we adopt the hyperparameters from (HSW$^+$22b), and for `Q3R` we cross-validate the learning rate and regularization hyperparameter λ. As shown

Table 3: GLUE Benchmark Scores

Method	MRPC	RTE	CoLA	STS-B	SST-2	QQP	MNLI	QNLI	Average
Dense Fine-tuning	91.9	**77.62**	62.3	**90.19**	94.04	90.2	**87.3**	91.49	**85.88**
LoRA rank=4	89.04	73.55	56.25	89.86	**94.3**	90.11	87.00	**92.5**	84.58
Q3R rank=4	**92.24**	77.23	**63.50**	**90.19**	92.2	**91.60**	87.2	90.20	85.86

in Table 3, Q3R matches or exceeds LoRA's accuracy on most tasks and exhibits a performance closer to dense fine-tuning. These results demonstrate that Q3R can serve as a unified, low-rank training strategy—both for pre-training and fine-tuning of Transformer models. We discuss additional fine-tuning experiments in Appendix D.2.

6 Limitations

While our experiments showcase a robust post-truncation accuracy of Q3R-trained Transformers on vision and natural language tasks in small-to-medium scale settings that exceeds (or in the case of fine-tuning, matches) the one of other relevant low-rank training paradigms, the viability of Q3R is yet to be established across diverse architectures and large-scale problems. Fundamentally, Q3R relies on a suitable choice of the regularization strength hyper parameter λ, as well as on a suitable choice of the target rank r_{target}. We provide ablations about these values in Appendix E.1. While Q3R exhibits vulnerability to elevated values of λ due to a convergence to a trivial, very low-rank matrix, this is easily detectable by monitoring the tail ratio $T(X, r) = \frac{\sum_{i=1}^{r} \sigma_i^2}{\|X\|_F^2}$ on models. In practice, we have observed stable behavior within the range $\lambda \in [0.001, 0.01]$. The target rank r_{target} remains insensitive to underestimation because of the direct computation of epsilon resulting in a large ϵ, and due to the monotonicity of the smoothing parameter update function (7), ϵ remains within a reasonable bound. We note that for weight matrices and iterations with large ϵ, the effect of AdamQ3R resembles the one of AdamW with weight decay parameter λ (see also (6)).

Arguably, a limitation of this work is also the fact that while the final weights after training are (for appropriate parameters) low-rank, AdamQ3R still handles *dense* weight matrix variables throughout training, which does not allow a reduction of the parameter budget *during* training, unlike recent work (MHP25). More elaborate post-training postprocessing (e.g., inspired by (WAUc$^+$23)) might lead to further performance improvements.

7 Conclusion

We introduced *Quadratic Reweighted Rank Regularization* (Q3R), a principled, optimizer-compatible framework for inducing low-rank structure in deep neural network weights through explicit, continuous regularization. By majorizing a smoothed log-determinant surrogate with a quadratic model embedded in the AdamQ3R optimizer, Q3R trains weight matrices to achieve target ranks with minimal accuracy loss. This enables model compression with negligible performance degradation under reasonable parameter reductions, decreasing deployment costs and increasing throughput. Our experimental results demonstrate that Q3R generalizes across modalities and training regimes, with its design being particularly suitable for low-rank pre-training. Reducing Q3R's computational overhead, for example via low-rank subspace projections, remains to future work.

Acknowledgement

We would like to thank Tonmoy Hasan and Arkaprava Sinha for their assistance in setting up the LLM experiments. I.G. and C.K acknowledge the support of the NSF Grant CCF-2549926 for this work.

References

[A+14] K. D. B. J. Adam et al. A method for stochastic optimization. *arXiv preprint arXiv:1412.6980*, 1412(6), 2014.

[AS17] J. M. Alvarez and M. Salzmann. Compression-aware training of deep networks. *Advances in neural information processing systems*, 30, 2017.

[AZW] I. Alkhouri, X. Zhang, and R. Wang. Structure-Preserving Network Compression Via Low-Rank Induced Training Through Linear Layers Composition. *Transactions on Machine Learning Research*.

[Bec17] A. Beck. *First-Order Methods in Optimization*. Society for Industrial and Applied Mathematics, Philadelphia, PA, 2017.

[BM03] S. Burer and R. D. Monteiro. A nonlinear programming algorithm for solving semidefinite programs via low-rank factorization. *Mathematical Programming*, 95(2):329–357, 2003.

[BS15] A. Beck and S. Sabach. Weiszfeld's Method: Old and New Results. *J. Optim. Theory Appl.*, 164(1):1–40, 2015.

[BV04] S. P. Boyd and L. Vandenberghe. *Convex optimization*. Cambridge university press, 2004.

[CC18] Y. Chen and Y. Chi. Harnessing Structures in Big Data via Guaranteed Low-Rank Matrix Estimation: Recent Theory and Fast Algorithms via Convex and Nonconvex Optimization. *IEEE Signal Process. Mag.*, 35(4):14–31, 2018.

[CESV13] E. J. Candès, Y. Eldar, T. Strohmer, and V. Voroninski. Phase Retrieval via Matrix Completion. *SIAM J. Imag. Sci.*, 6(1):199–225, 2013.

[CLC19] Y. Chi, Y. M. Lu, and Y. Chen. Nonconvex Optimization Meets Low-Rank Matrix Factorization: An Overview. *IEEE Trans. Signal Process.*, 67(20):5239–5269, 2019.

[CR09] E. J. Candès and B. Recht. Exact matrix completion via convex optimization. *Found. Comput. Math.*, 9(6):717–772, 2009.

[CW18] J.-F. Cai and K. Wei. Exploiting the Structure Effectively and Efficiently in Low-Rank Matrix Recovery. *Processing, Analyzing and Learning of Images, Shapes, and Forms*, 19:21 pp., 2018.

[CZM+19] E. D. Cubuk, B. Zoph, D. Mane, V. Vasudevan, and Q. V. Le. AutoAugment: Learning Augmentation Policies from Data. 2019.

[DBKea21] A. Dosovitskiy, L. Beyer, A. Kolesnikov, and et al. An Image is Worth 16x16 Words: Transformers for Image Recognition at Scale. In *ICLR*, 2021.

[DCLT19] J. Devlin, M.-W. Chang, K. Lee, and K. Toutanova. BERT: Pre-training of Deep Bidirectional Transformers for Language Understanding. In J. Burstein, C. Doran, and T. Solorio, editors, *Proceedings of the 2019 Conference of the North American Chapter of the Association for Computational Linguistics: Human Language Technologies, Volume 1 (Long and Short Papers)*, pages 4171–4186, Minneapolis, Minnesota, June 2019. Association for Computational Linguistics.

[DCM22] F. Dörfler, J. Coulson, and I. Markovsky. Bridging direct and indirect data-driven control formulations via regularizations and relaxations. *IEEE Transactions on Automatic Control*, 68(2):883–897, 2022.

[DR16] M. A. Davenport and J. Romberg. An Overview of Low-Rank Matrix Recovery From Incomplete Observations. *IEEE J. Sel. Topics Signal Process.*, 10:608–622, 2016.

[ETK+25] A. Edalati, M. Tahaei, I. Kobyzev, V. P. Nia, J. J. Clark, and M. Rezagholizadeh. KronA: Parameter-Efficient Tuning with Kronecker Adapter. In *Enhancing LLM Performance: Efficacy, Fine-Tuning, and Inference Techniques*, pages 49–65. Springer, 2025.

[FHB03] M. Fazel, H. Hindi, and S. P. Boyd. Log-det heuristic for matrix rank minimization with applications to Hankel and Euclidean distance matrices. In *Proceedings of the American Control Conference*, volume 3, pages 2156–2162, 2003.

[FHB04] M. Fazel, H. A. Hindi, and S. P. Boyd. Rank Minimization and Applications in System Theory. In *Proceedings of the American Control Conference*, number 4, pages 3273–3278, 2004.

[FRW11] M. Fornasier, H. Rauhut, and R. Ward. Low-rank Matrix Recovery via Iteratively Reweighted Least Squares Minimization. *SIAM J. Optim.*, 21(4):1614–1640, 2011.

[GK+22] A. N. Gomez, S. R. Kamalakara, et al. Exploring Low Rank Training of Deep Neural Networks. *arXiv preprint arXiv:2209.13569*, 2022.

[GSGP25] T. Galanti, Z. S. Siegel, A. Gupte, and T. A. Poggio. SGD with weight decay secretly minimizes the ranks of your neural networks. In *The Second Conference on Parsimony and Learning (CPAL 2025)*, 2025.

[GTK24] I. Ghosh, A. Tasissa, and C. Kümmerle. Sample-Efficient Geometry Reconstruction from Euclidean Distances using Non-Convex Optimization. In A. Globerson, L. Mackey, D. Belgrave, A. Fan, U. Paquet, J. Tomczak, and C. Zhang, editors, *Advances in Neural Information Processing Systems*, volume 37, pages 77226–77268. Curran Associates, Inc., 2024.

[HGJ+19] N. Houlsby, A. Giurgiu, S. Jastrzebski, B. Morrone, Q. De Laroussilhe, A. Gesmundo, M. Attariyan, and S. Gelly. Parameter-efficient transfer learning for NLP. In *International conference on machine learning*, pages 2790–2799. PMLR, 2019.

[HMT11] N. Halko, P.-G. Martinsson, and J. A. Tropp. Finding structure with randomness: Probabilistic algorithms for constructing approximate matrix decompositions. *SIAM Review*, 53(2):217–288, 2011.

[HMZ+23] M. Huh, H. Mobahi, R. Zhang, B. Cheung, P. Agrawal, and P. Isola. The Low-Rank Simplicity Bias in Deep Networks. *Transactions on Machine Learning Research*, 2023.

[HSW+22a] E. J. Hu, Y. Shen, P. Wallis, Z. Allen-Zhu, Y. Li, S. Wang, L. Wang, and W. Chen. LoRA: Low-Rank Adaptation of Large Language Models. In *ICLR*, 2022.

[HSW+22b] E. J. Hu, Y. Shen, P. Wallis, Z. Allen-Zhu, Y. Li, S. Wang, L. Wang, W. Chen, et al. Lora: Low-rank adaptation of large language models. *ICLR*, 1(2):3, 2022.

[HUSN84] J.-B. Hiriart-Urruty, J.-J. Strodiot, and V. H. Nguyen. Generalized Hessian matrix and second-order optimality conditions for problems with $C^{1,1}$ data. *Appl. Math. Optim.*, 11(1):43–56, 1984.

[KBV09] Y. Koren, R. Bell, and C. Volinsky. Matrix Factorization Techniques for Recommender Systems. *Computer*, 42(8):30–37, 2009.

[KJP+25] O. Khade, S. Jagdale, A. Phaltankar, G. Takalikar, and R. Joshi. Challenges in Adapting Multilingual LLMs to Low-Resource Languages using LoRA PEFT Tuning. In *Proceedings of the First Workshop on Challenges in Processing South Asian Languages (CHiPSAL 2025)*, pages 217–222, Abu Dhabi, UAE, 2025. International Committee on Computational Linguistics.

[KM23] C. Kümmerle and J. Maly. Recovering simultaneously structured data via non-convex iteratively reweighted least squares. *Advances in Neural Information Processing Systems (NeurIPS 2023)*, 36:71799–71833, 2023.

[KMV21] C. Kümmerle and C. Mayrink Verdun. A scalable second order method for ill-conditioned matrix completion from few samples. In *ICML 2021*, pages 5872–5883, 2021.

[Kor09] Y. Koren. The BellKor Solution to the Netflix Grand Prize. *Netflix prize documentation*, 81(2009):1–10, 2009.

[Kri09] A. Krizhevsky. Learning Multiple Layers of Features from Tiny Images. *BibSonomy*, pages 32–33, 2009.

[KS18] C. Kümmerle and J. Sigl. Harmonic Mean Iteratively Reweighted Least Squares for Low-Rank Matrix Recovery. *J. Mach. Learn. Res.*, 19(47):1–49, 2018.

[KTMF21] S. Kamalakara, N. Tenenholtz, L. Mackey, and N. Fusi. Initialization and Regularization of Factorized Neural Layers. In *International Conference on Learning Representations (ICLR 2021)*, 2021.

[Lew95] A. S. Lewis. The Convex Analysis of Unitarily Invariant Matrix Functions. *J. Convex Anal.*, 2(1–2):173–183, 1995.

[LFX+24] A. Liu, B. Feng, B. Xue, B. Wang, B. Wu, C. Lu, C. Zhao, C. Deng, C. Zhang, C. Ruan, et al. DeepSeek-V3 Technical Report. *CoRR*, abs/2412.19437, 2024.

[LH19] I. Loshchilov and F. Hutter. Decoupled Weight Decay Regularization. In *International Conference on Learning Representations (ICLR 2019)*, 2019.

[LHLZ24] Y. Luo, W. Huang, X. Li, and A. Zhang. Recursive importance sketching for rank constrained least squares: Algorithms and high-order convergence. *Operations Research*, 72(1):237–256, 2024.

[LS05] A. S. Lewis and H. S. Sendov. Nonsmooth Analysis of Singular Values. Part I: Theory. *Set-Valued Analysis*, 13(3):213–241, 2005.

[LSMR23] V. Lialin, N. Shivagunde, S. Muckatira, and A. Rumshisky. ReLoRA: High-Rank Training Through Low-Rank Updates. In *Workshop on Advancing Neural Network Training at 37th Conference on Neural Information Processing Systems (WANT@NeurIPS 2023)*, 2023.

[LWY+24] S.-Y. Liu, C.-Y. Wang, H. Yin, P. Molchanov, Y.-C. F. Wang, K.-T. Cheng, and M.-H. Chen. Dora: Weight-decomposed low-rank adaptation. In *Forty-first International Conference on Machine Learning*, 2024.

[MF10] K. Mohan and M. Fazel. Reweighted nuclear norm minimization with application to system identification. In *Proceedings of the American Control Conference*, pages 2953–2959. IEEE, 2010.

[MHP25] Z. Mo, L.-K. Huang, and S. J. Pan. Parameter and memory efficient pretraining via low-rank riemannian optimization. In *The Thirteenth International Conference on Learning Representations (ICLR 2025)*, 2025.

[MHR21] R. K. Mahabadi, J. Henderson, and S. Ruder. COMPACTER: efficient low-rank hypercomplex adapter layers. In *Proceedings of the 35th International Conference on Neural Information Processing Systems*, NIPS '21, Red Hook, NY, USA, 2021. Curran Associates Inc.

[MNA+18] P. Micikevicius, S. Narang, J. Alben, G. Diamos, E. Elsen, D. Garcia, B. Ginsburg, M. Houston, O. Kuchaiev, G. Venkatesh, and H. Wu. Mixed Precision Training. 2018.

[MWCC20] C. Ma, K. Wang, Y. Chi, and Y. Chen. Implicit Regularization in Nonconvex Statistical Estimation: Gradient Descent Converges Linearly for Phase Retrieval, Matrix Completion, and Blind Deconvolution. *Foundations of Computational Mathematics*, 20:451–632, 2020.

[Nat95] B. Natarajan. Sparse Approximate Solutions to Linear Systems. *SIAM J. Comput.*, 24(2):227–234, 1995.

[RBD25] A. Radhakrishnan, M. Belkin, and D. Drusvyatskiy. Linear Recursive Feature Machines provably recover low-rank matrices. *Proceedings of the National Academy of Sciences*, 122(13):e2411325122, 2025.

[RFP10] B. Recht, M. Fazel, and P. A. Parrilo. Guaranteed Minimum-Rank Solutions of Linear Matrix Equations via Nuclear Norm Minimization. *SIAM Review*, 52(3):471–501, 2010.

[RKZK22] S. Rendle, W. Krichene, L. Zhang, and Y. Koren. Revisiting the Performance of iALS on Item Recommendation Benchmarks. In *Proceedings of the 16th ACM Conference on Recommender Systems*, RecSys '22, page 427–435. Association for Computing Machinery, 2022.

[RWC+19] A. Radford, J. Wu, R. Child, D. Luan, D. Amodei, and I. Sutskever. Language Models are Unsupervised Multitask Learners. *OpenAI Blog*, 2019. Technical report.

[SKZ+22] A. P. Steiner, A. Kolesnikov, X. Zhai, R. Wightman, J. Uszkoreit, and L. Beyer. How to train your ViT? Data, Augmentation, and Regularization in Vision Transformers. *Transactions on Machine Learning Research*, 2022.

[SL16] R. Sun and Z. Q. Luo. Guaranteed Matrix Completion via Non-Convex Factorization. *IEEE Trans. Inf. Theory*, 62(11):6535–6579, 2016.

[SZ25] D. Stöger and Y. Zhu. Non-convex matrix sensing: Breaking the quadratic rank barrier in the sample complexity. In N. Haghtalab and A. Moitra, editors, *Proceedings of the 38th Annual Conference on Learning Theory*, volume 291 of *Proceedings of Machine Learning Research*, pages 1–2. PMLR, 2025.

[SZCT23] D. Savostianova, E. Zangrando, G. Ceruti, and F. Tudisco. Robust Low-Rank Training via Orthonormal Constraints. In *Advances in Neural Information Processing Systems (NeurIPS)*, 2023.

[WAUc+23] H. Wang, S. Agarwal, P. U-chupala, Y. Tanaka, E. Xing, and D. Papailiopoulos. Cuttlefish: Low-Rank Model Training without All the Tuning. In D. Song, M. Carbin, and T. Chen, editors, *Proceedings of Machine Learning and Systems (MLSys 2023)*, volume 5, pages 578–605. Curan, 2023.

[Wei37] E. Weiszfeld. Sur le point pour lequel la somme des distances de n points donnés est minimum. *Tohoku Mathematical Journal, First Series*, 43:355–386, 1937.

[WMPG24a] X. Wei, S. Moalla, R. Pascanu, and C. Gulcehre. Building on Efficient Foundations: Effective Training of LLMs with Structured Feedforward Layers. In *Advances in Neural Information Processing Systems (NeurIPS 2024)*, volume 37, pages 4689–4717, 2024.

[WMPG24b] X. Wei, S. Moalla, R. Pascanu, and C. Gulcehre. Investigating Low-Rank Training in Transformer Language Models: Efficiency and Scaling Analysis. In *ICML 2024 Workshop on "Next Generation of Sequence Modeling Architectures"*, 2024.

[WP09] E. Weiszfeld and F. Plastria. On the point for which the sum of the distances to n given points is minimum. *Ann. Oper. Res.*, 167(1):7–41, Mar 2009.

[XLZ+20] Y. Xu, Y. Li, S. Zhang, W. Wen, B. Wang, Y. Qi, Y. Chen, W. Lin, and H. Xiong. TRP: Trained Rank Pruning for Efficient Deep Neural Networks. In C. Bessiere, editor, *Proceedings of the Twenty-Ninth International Joint Conference on Artificial Intelligence, IJCAI-20*, pages 977–983. International Joint Conferences on Artificial Intelligence Organization, 7 2020. Main track.

[XSCM23] X. Xu, Y. Shen, Y. Chi, and C. Ma. The power of preconditioning in overparameterized low-rank matrix sensing. In *International Conference on Machine Learning*, pages 38611–38654. PMLR, 2023.

[YATC20] H. Yang, P. Antonante, V. Tzoumas, and L. Carlone. Graduated Non-Convexity for Robust Spatial Perception: From Non-Minimal Solvers to Global Outlier Rejection. *IEEE Robotics and Automation Letters*, 5(2):1127–1134, 2020.

[YCS+20] F. Yang, X. Chen, W. Shao, S.-F. Chang, and W. Liu. Learning Low-Rank Deep Neural Networks via Singular Vector Decomposition. In *IEEE/CVF Conference on Computer Vision and Pattern Recognition Workshops (CVPRW)*, pages 954–963, 2020.

[YTW+20] H. Yang, M. Tang, W. Wen, F. Yan, D. Hu, A. Li, H. Li, and Y. Chen. Learning Low-Rank Deep Neural Networks via Singular Vector Orthogonality Regularization and Singular Value Sparsification. In *Proceedings of the IEEE/CVF Conference on Computer Vision and Pattern Recognition (CVPR) Workshops*, June 2020.

[YYT+20] F. Yan, Y. Yang, Y. Tang, et al. Learning Low-Rank Deep Neural Networks via Singular Vector Decomposition. In *Proceedings of the IEEE/CVF Conference on Computer Vision and Pattern Recognition Workshops (CVPRW)*, 2020.

[ZCZ22] J. Zhang, H.-M. Chiu, and R. Y. Zhang. Accelerating SGD for Highly Ill-Conditioned Huge-Scale Online Matrix Completion. *NeurIPS*, 35:37549–37562, 2022.

[ZHSJ20] J. Zhang, T. He, S. Sra, and A. Jadbabaie. Why gradient clipping accelerates training: A theoretical justification for adaptivity, 2020.

[ZL15] Q. Zheng and J. Lafferty. A Convergent Gradient Descent Algorithm for Rank Minimization and Semidefinite Programming from Random Linear Measurements. In *Advances in Neural Information Processing Systems (NIPS)*, pages 109–117, 2015.

[ZN22] P. Zilber and B. Nadler. GNMR: a provable one-line algorithm for low rank matrix recovery. *SIAM J. Math. Data Sci.*, 4(2):909–934, 2022.

[ZZC+24] J. Zhao, Z. Zhang, B. Chen, Z. Wang, A. Anandkumar, and Y. Tian. GaLore: Memory-Efficient LLM Training by Gradient Low-Rank Projection. *ICML*, 2024.

Supplementary material for *Q3R: Quadratic Reweighted Rank Regularizer for Effective Low-Rank Training*

In this supplementary material, we first provide theoretical justifications of the relationship between Q3R and the smoothed objective, expanding on Section 4.1, in Appendix A. The derivation of a Q3Rvalue evaluation algorithm is provided in Appendix B. The expression used in AdamQ3R is derived in Appendix C. In Appendix D, we discuss more experimental results in both pre-training and fine-tuning, and we discuss the computational aspects. In the concluding part of this supplementary material, in Appendix E, we demonstrate the robustness of Q3R to hyperparameter variation.

A Relationship between Smoothed Log-Determinant and Q3R

In this section, we expand on the relationship between the ϵ-smoothed log-determinant surrogate objective $F_\epsilon(\cdot)$ defined in (1). Part of this material is covered in (KM23, Section B.2) in a different context.

A.1 Properties of Smoothed Log-Deteriminant

We focus first on some basic properties of the ϵ-smoothed log-determinant $F_\epsilon : \mathbb{R}^{d_1 \times d_2} \to \mathbb{R}$, which, as we recall from (1), was defined for any $\mathbf{W} \in \mathbb{R}^{d_1 \times d_2}$ as

$$F_\epsilon(\mathbf{W}) := \sum_{i=1}^{d} f_\epsilon(\sigma_i(\mathbf{W})), \text{ where } f_\epsilon(\sigma) = \begin{cases} \epsilon^2 \left(\log(\sigma) - \log(\epsilon)\right) + \frac{1}{2}\epsilon^2, & \text{if } \sigma \geqslant \epsilon, \\ \frac{1}{2}\sigma^2, & \text{if } \sigma < \epsilon, \end{cases}$$

given $\epsilon > 0$.

As seen by its definition, $F_\epsilon(\cdot)$ is a *spectral function*, i.e., it only depends on the singular values $\sigma_1(\mathbf{W}), \sigma_2(\mathbf{W}), \ldots$ of $\mathbf{W}$, but not on any singular vector information.

Let now $d := \min(d_1, d_2)$. More precisely, we can define, following (Lew95; Bec17; LS05), a *spectral function* $F : \mathbb{R}^{d_1 \times d_2} \to \mathbb{R}$ as a function for which there exists a function $f : \mathbb{R}^d \to \mathbb{R}$ for which $F = f \circ \sigma$, where $\sigma : \mathbb{R}^{d_1 \times d_2} \to \mathbb{R}^d$, $\mathbf{W} \mapsto \sigma(\mathbf{W}) = (\sigma_1(\mathbf{W}), \ldots, \sigma_d(\mathbf{W}))$ is the function mapping matrices in $\mathbb{R}^{d_1 \times d_2}$ to its singular value vector $\sigma(\mathbf{W})$. A key towards understanding the derivative structure is that we can obtain an explicit formula for the gradient $\nabla F(\mathbf{W})$ of F_ϵ at $\mathbf{W}$ if the function f in the spectral function definition is absolutely (permutation) symmetric (Bec17, Section 7.3) according to Definition A.1. It is easy to check that f_ϵ from the definition of the ϵ-smoothed log-determinant $F_\epsilon(\cdot)$ satisfies this definition.

Definition A.1 (Absolutely permutation symmetric functions)**.**

1. *Let $\mathbf{x} \in \mathbb{R}^d$. We call $r(\mathbf{x}) \in \mathbb{R}^d$ the* non-increasing rearrangement *of $\mathbf{x}$ if it holds that*

$$r(\mathbf{x})_1 \geqslant r(\mathbf{x})_2 \geqslant \ldots \geqslant r(\mathbf{x})_d$$

and there is a permutation matrix $\mathbf{P} \in \mathbb{P}^d$ such that $r(\mathbf{x})_i = (\mathbf{P}\mathbf{x})_i$ for all $i \in [d]$.

2. *We say that a function $f : \mathbb{R}^d \to \mathbb{R}$ is* absolutely permutation symmetric *if*

$$f(\mathbf{x}) = f(r(|\mathbf{x}|)) \tag{8}$$

for any $\mathbf{x} \in \mathbb{R}^d$.

For ease of notation, given a vector $\mathbf{v} \in \mathbb{R}^d$, we define $\mathrm{dg}(\mathbf{v}) \in \mathbb{R}^{d_1 \times d_2}$ be the rectangular diagonal matrix such that for $v \in \mathbb{R}^d$ and any $i \in \{1, \ldots, d_1\}$, $j \in \{1, \ldots, d_2\}$,

$$\mathrm{dg}(\mathbf{v})_{ij} = \begin{cases} \mathbf{v}_i, & \text{if } i = j, \\ 0, & \text{else.} \end{cases}$$

Next, we cite a key result about the differentiability of spectral functions which is due to

Proposition A.1 (Differentiability of Spectral Functions (LS05, Section 7))**.** *Let $F : \mathbb{R}^{d_1 \times d_2} \to \mathbb{R}$ be a spectral function $F = f \circ \sigma$ with an associated function $f : \mathbb{R}^d \to \mathbb{R}$ that is absolutely permutation symmetric. Then, F is differentiable at $\mathbf{W} \in \mathbb{R}^{d_1 \times d_2}$ if and only if f is differentiable at $\sigma(\mathbf{W}) \in \mathbb{R}^d$.*

In this case, the gradient ∇F of F at $\mathbf{W}$ is given by

$$\nabla F(\mathbf{W}) = \mathbf{U} \,\mathrm{dg}\left(\nabla f(\sigma(\mathbf{W})\right) \mathbf{V}^\top$$

if $\mathbf{W} = \mathbf{U} \,\mathrm{dg}\left(\sigma(\mathbf{W})\right) \mathbf{V}^\top$ is a singular value decomposition of $\mathbf{W}$ with orthogonal matrices $\mathbf{U} \in \mathbb{R}^{d_1 \times d_1}$ and $\mathbf{V} \in \mathbb{R}^{d_2 \times d_2}$.

Using Proposition A.1, we can characterize the derivative of the F_ϵ for arbitrary $\epsilon > 0$, as established in the following lemma.

Lemma A.2. *Let $\epsilon > 0$ and $F_\epsilon : \mathbb{R}^{d_1 \times d_2} \to \mathbb{R}$ be the ϵ-smoothed log-determinant of Equation* (1)*. Then F_ϵ is differentiable with 1-Lipschitz gradient $\nabla F_\epsilon : \mathbb{R}^{d_1 \times d_2} \to \mathbb{R}^{d_1 \times d_2}$ that is given by*

$$\nabla F_\epsilon(\mathbf{W}) = \mathbf{U}_\mathbf{W} \,\mathrm{dg}\left(\frac{\sigma_i(\mathbf{W})}{\max(\sigma_i(\mathbf{W})/\epsilon, 1)^2}\right)_{i=1}^d \mathbf{V}_\mathbf{W}^\top \tag{9}$$

for any matrix $\mathbf{W}$ with singular value decomposition $\mathbf{W} = \mathbf{U}_\mathbf{W} \,\mathrm{dg}\left(\sigma(\mathbf{W})\right) \mathbf{V}_\mathbf{W}^\top = \mathbf{U}_\mathbf{W} \,\mathrm{dg}\left(\sigma\right) \mathbf{V}_\mathbf{W}^\top$.

Proof of Lemma A.2. For the differentiability of F_ϵ, as per Proposition A.1, it is sufficient to show that the function $f((\sigma_1, \ldots, \sigma_d)) = \sum_{i=1}^d f_\epsilon(\sigma_i)$ with $f_\epsilon : \mathbb{R}_{\geqslant 0} \to \mathbb{R}$ as defined in (1) is differentiable at any $(\sigma_1, \ldots, \sigma_d) \in \mathbb{R}^d_{\geqslant 0}$. Due to the sum structure of f, this will follow if f_ϵ is itself differentiable at any $\sigma \geqslant 0$.

To this, we observe that for any $\sigma > 0, \sigma \neq \epsilon$, we have that f_ϵ is differentiable at σ with derivative

$$f_\epsilon'(\sigma) = \begin{cases} \frac{\epsilon^2}{\sigma}, & \text{if } \sigma > \epsilon \\ \sigma, & \text{if } 0 \leqslant \sigma < \epsilon. \end{cases}$$

Since $\lim_{\sigma \nearrow \epsilon} f_\epsilon'(\sigma) = \epsilon = \lim_{\sigma \searrow \epsilon} f_\epsilon'(\sigma)$, it follows that f_ϵ is also differentiable at $\sigma = \epsilon$ with $f_\epsilon'(\epsilon) = \epsilon$, and thus, differentiable on the entirety of its domain. The formula (9) follows then directly from Proposition A.1. ☐

Remark A.3. It is well-known that the optimization of *convex* functions (BV04) is from many perspectives less challenging than the optimization of non-convex functions. In Section 4.1, we have claimed that the ϵ-smoothed log-determinant surrogate is *not* convex. This can indeed by shown directly by invoking (LS05, Proposition 6.1), which states that a spectral function $F = f \circ \sigma$ is convex if and only if f is convex. Indeed, it is easy to see that $f_\epsilon(\cdot)$ is not convex due to its logarithmic dependence on the input for large inputs, which shows that $F_\epsilon(\cdot)$ is not a convex function.

As mentioned in Section 4.1, we see from (9) that computing $\nabla F_\epsilon(\mathbf{W})$ given the matrix $\mathbf{W} \in \mathbb{R}^{d_1 \times d_2}$ indeed would require a *full* singular value decomposition that includes at least d leading singular values. Defining $r(\mathbf{W}, \epsilon) := |\{i \in \{1, \ldots, d\} : \sigma_i(\mathbf{W}) > \epsilon\}|$ as in (3) and $\Sigma = \mathrm{diag}(\sigma_i(\mathbf{W}))_{i=1}^{r(\mathbf{W},\epsilon)} \in \mathbb{R}^{r(\mathbf{W},\epsilon)\times r(\mathbf{W},\epsilon)}$ as in (4), we obtain for $\mathbf{U}$ and $\mathbf{V}$ defined from the $r(\mathbf{W}, \epsilon)$ leading columns of $\mathbf{U_W} = [\mathbf{U} \quad \mathbf{U}_\perp] \in \mathbb{R}^{d_1 \times d_1}$ and $\mathbf{V_W} = [\mathbf{V} \quad \mathbf{V}_\perp] \in \mathbb{R}^{d_2 \times d_2}$ that

$$\nabla F_\epsilon(\mathbf{W}) = \epsilon^2 \mathbf{U}\Sigma^{-1}\mathbf{V}^\top + \mathbf{U}_\perp \Sigma_\perp \mathbf{V}_\perp^\top, \tag{10}$$

inserting the formula from (9), with the notation that $\Sigma_\perp = \mathrm{dg}\left(\sigma_i(\mathbf{W})\right)_{i=r(\mathbf{W},\epsilon)+1}^{d}$. Fundamentally, this is the key reason why a direct inclusion of the smoothed log-determinant objective into a gradient-based optimization algorithm is computationally inefficient.

Finally, we conclude with the observation that $F_\epsilon(\cdot)$ becomes *convex* if $\epsilon \gg 0$ is chosen large enough. In particular, it holds for any $\mathbf{W} \in \mathbb{R}^{d_1 \times d_2}$ that

$$F_\epsilon(\mathbf{W}) = \sum_{i=1}^{d} f_\epsilon(\sigma_i(\mathbf{W})) = \sum_{i=1}^{d} \frac{1}{2}\sigma_i^2(\mathbf{W}) = \frac{1}{2}\|\mathbf{W}\|_F^2$$

if additionally the largest singular value $\sigma_1(\mathbf{W})$ of $\mathbf{W}$ satisfies $\sigma_1(\mathbf{W}) \leqslant \epsilon$. Here, we used in the last equality that the Frobenius norm of a matrix is the ℓ_2-norm if its singular values.

A.2 The Quadratic Model Function Underlying `Q3R`

We proceed by justifying the claims made in Section 4.1 about the relationship between the ϵ-smoothed log-determinant $F_\epsilon(\cdot)$, the `Q3R`-regularizer $\mathrm{Q3R}_{\mathbf{W}',\epsilon}(\cdot)$, the quadratic model $Q_\epsilon(\cdot \mid \mathbf{W}')$ of (2) and the reweighting operator $\mathcal{R}_{\mathbf{W}',\epsilon}(\cdot)$. To this end, we show the first statements of Lemma A.2 that characterize the reweighting operator $\mathcal{R}_{\mathbf{W}',\epsilon}(\cdot)$.

Proof of Lemma 4.1.1. Let $\mathbf{W}' \in \mathbb{R}^{d_1 \times d_2}$ be arbitrary with singular value decomposition $\mathbf{W}' = \mathbf{U}' \,\mathrm{dg}(\sigma_i(\mathbf{W}'))\mathbf{V}'^\top$. Recall from Definition 4.1 that

$$\mathcal{R}_{\mathbf{W}',\epsilon}(\mathbf{W}) = \mathbf{U}'\Sigma_{\epsilon,d_1}^{-1}\mathbf{U}'^\top\mathbf{W}\mathbf{V}'\Sigma_{\epsilon,d_2}^{-1}\mathbf{V}'^\top,$$

where $\Sigma_{\epsilon,d} = \mathrm{diag}(\max(\sigma_i(\mathbf{W}')/\epsilon, 1))_{i=1}^{d} \in \mathbb{R}^{d\times d}$ for $d \in \{d_1, d_2\}$.

To show that $\mathcal{R}_{\mathbf{W}',\epsilon} : \mathbb{R}^{d_1\times d_2} \to \mathbb{R}^{d_1\times d_2}$ is a positive definite operator, we consider any $\mathbf{W} \in \mathbb{R}^{d_1\times d_2}$ such that $\mathbf{W} \neq 0$, which implies that $\|\mathbf{W}\|_F > 0$. Defining $\mathbf{Z} := \mathbf{U}'^\top\mathbf{W}\mathbf{V}'$, we see that

$$\begin{aligned}
\langle \mathbf{W}, \mathcal{R}_{\mathbf{W}',\epsilon}(\mathbf{W})\rangle &= \mathrm{tr}\left(\mathbf{W}^\top\mathcal{R}_{\mathbf{W}',\epsilon}(\mathbf{W})\right) = \mathrm{tr}\left(\mathbf{W}^\top\mathbf{U}'\Sigma_{\epsilon,d_1}^{-1}\mathbf{U}'^\top\mathbf{W}\mathbf{V}'\Sigma_{\epsilon,d_2}^{-1}\mathbf{V}'^\top\right) \\
&= \mathrm{tr}\left(\mathbf{V}'^\top\mathbf{W}^\top\mathbf{U}'\Sigma_{\epsilon,d_1}^{-1}\mathbf{U}'^\top\mathbf{W}\mathbf{V}'\Sigma_{\epsilon,d_2}^{-1}\right) = \mathrm{tr}\left(\mathbf{Z}^\top\Sigma_{\epsilon,d_1}^{-1}\mathbf{Z}\Sigma_{\epsilon,d_2}^{-1}\right) \\
&= \mathrm{tr}\left((\Sigma_{\epsilon,d_1}^{-1}\mathbf{Z})^\top\mathbf{Z}\Sigma_{\epsilon,d_2}^{-1}\right) = \sum_{i=1}^{d_1}\sum_{j=1}^{d_2}(\Sigma_{\epsilon,d_1}^{-1}\mathbf{Z})_{ij}(\mathbf{Z}\Sigma_{\epsilon,d_2}^{-1})_{ij} \\
&= \sum_{i=1}^{d_1}\sum_{j=1}^{d_2}\widetilde{\sigma}_i\widetilde{\sigma}_j\mathbf{Z}_{ij}^2
\end{aligned}$$

with $\widetilde{\sigma}_i := \max(\sigma_i(\mathbf{W}')/\epsilon, 1)^{-1}$ for $i \in \{1, \ldots, \max(d_1, d_2)\}$, with using the cyclicity of the trace in the third equality. Since $\widetilde{\sigma}_i, \widetilde{\sigma}_j > 0$ for all i, j, we can establish the lower bound

$$\begin{aligned}
\langle \mathbf{W}, \mathcal{R}_{\mathbf{W}',\epsilon}(\mathbf{W})\rangle &= \sum_{i=1}^{d_1}\sum_{j=1}^{d_2}\widetilde{\sigma}_i\widetilde{\sigma}_j \geqslant \min_{i=1}^{\max(d_1,d_2)}\widetilde{\sigma}_i^2\sum_{i=1}^{d_1}\sum_{j=1}^{d_2}\mathbf{Z}_{ij}^2 = \min_{i=1}^{\max(d_1,d_2)}\widetilde{\sigma}_i^2\|\mathbf{Z}\|_F^2 \\
&= \min_{i=1}^{\max(d_1,d_2)}\widetilde{\sigma}_i^2\|\mathbf{U}'^\top\mathbf{W}\mathbf{V}'\|_F^2 = \min_{i=1}^{\max(d_1,d_2)}\widetilde{\sigma}_i^2\|\mathbf{W}\|_F^2 > 0.
\end{aligned}$$

□

Due to the definition of Q3R (6), an implication of this is that

$$\mathrm{Q3R}_{\mathbf{W}',\epsilon}(\mathbf{W}) = \frac{1}{2}\langle \mathbf{W}, \mathcal{R}_{\mathbf{W}',\epsilon}(\mathbf{W})\rangle \geqslant 0$$

and $\mathrm{Q3R}_{\mathbf{W}',\epsilon}(\mathbf{W}) = 0 \Leftrightarrow \mathbf{W} = 0$, i.e., the value of Q3R is always non-negative and positive for non-zero matrices.

We proceed with the proof of the second statement of Lemma 4.1, which provides an explicit formula for the reweighting operator that only requires a partial SVD of $\mathbf{W}'$.

Proof of Lemma 4.1.2. If $\mathbf{W}' = \mathbf{U}_{\mathbf{W}'} \operatorname{dg}(\sigma_i(\mathbf{W}'))\mathbf{V}_{\mathbf{W}'}^\top$ is a full singular value decomposition of $\mathbf{W}'$ with $\mathbf{U}_{\mathbf{W}'} = [\mathbf{U} \quad \mathbf{U}_\perp] \in \mathbb{R}^{d_1 \times d_1}$ and $\mathbf{V}_{\mathbf{W}'} = [\mathbf{V} \quad \mathbf{V}_\perp] \in \mathbb{R}^{d_2 \times d_2}$, we recall that the image of a matrix $\mathbf{W} \in \mathbb{R}^{d_1 \times d_2}$ with respect to $\mathcal{R}_{\mathbf{W}',\epsilon}$ is defined (see Definition 4.1) as

$$\mathcal{R}_{\mathbf{W}',\epsilon}(\mathbf{W}) = \mathbf{U}_{\mathbf{W}'}\Sigma_{\epsilon,d_1}^{-1}\mathbf{U}_{\mathbf{W}'}^\top \mathbf{W}\mathbf{V}_{\mathbf{W}'}\Sigma_{\epsilon,d_2}^{-1}\mathbf{V}_{\mathbf{W}'}^\top, \tag{11}$$

using the definition for $\Sigma_{\epsilon,d}$ from the proof of Lemma 4.1.1 above.

With a similar argument as made in (10), we can see that

$$\mathbf{U}_{\mathbf{W}'}\Sigma_{\epsilon,d_1}^{-1}\mathbf{U}_{\mathbf{W}'}^\top = \epsilon\mathbf{U}\Sigma^{-1}\mathbf{U}^\top + \mathbf{U}_\perp\mathbf{U}_\perp^\top = \epsilon\mathbf{U}\Sigma^{-1}\mathbf{U}^\top + \mathbf{I} - \mathbf{U}\mathbf{U}^\top$$

with $\Sigma = \operatorname{diag}(\sigma_i(\mathbf{W}'))_{i=1}^{r(\mathbf{W}',\epsilon)} \in \mathbb{R}^{r(\mathbf{W}',\epsilon)\times r(\mathbf{W}',\epsilon)}$, $\mathbf{U} \in \mathbb{R}^{d_1 \times r(\mathbf{W}',\epsilon)}$ and the identity matrix $\mathbf{I}$. In the last equation, we used that $\mathbf{U}_\perp\mathbf{U}_\perp^\top$ is the projection operator onto the subspace that is *orthogonal* to the one spanned by the columns of $\mathbf{U}$. Analogously, we obtain that

$$\mathbf{V}_{\mathbf{W}'}\Sigma_{\epsilon,d_2}^{-1}\mathbf{V}_{\mathbf{W}'}^\top = \epsilon\mathbf{V}\Sigma^{-1}\mathbf{V}^\top + \mathbf{V}_\perp\mathbf{V}_\perp^\top = \epsilon\mathbf{V}\Sigma^{-1}\mathbf{V}^\top + \mathbf{I} - \mathbf{V}\mathbf{V}^\top,$$

where $\mathbf{V} \in \mathbb{R}^{d_2 \times r(\mathbf{W}',\epsilon)}$. Inserting these two equations into (11), we obtain

$$\begin{aligned}
\mathcal{R}_{\mathbf{W}',\epsilon}(\mathbf{W}) &= \mathbf{U}_{\mathbf{W}'}\Sigma_{\epsilon,d_1}^{-1}\mathbf{U}_{\mathbf{W}'}^\top \mathbf{W}\mathbf{V}_{\mathbf{W}'}\Sigma_{\epsilon,d_2}^{-1}\mathbf{V}_{\mathbf{W}'}^\top = \\
&= \left(\epsilon\mathbf{U}\Sigma^{-1}\mathbf{U}^\top + \mathbf{I} - \mathbf{U}\mathbf{U}^\top\right)\mathbf{W}\left(\epsilon\mathbf{V}\Sigma^{-1}\mathbf{V}^\top + \mathbf{I} - \mathbf{V}\mathbf{V}^\top\right) \\
&= \epsilon^2\mathbf{U}\Sigma^{-1}\mathbf{U}^\top\mathbf{W}\mathbf{V}\Sigma^{-1}\mathbf{V}^\top + \epsilon\mathbf{U}\Sigma^{-1}\mathbf{U}^\top\mathbf{W}\left(\mathbf{I} - \mathbf{V}\mathbf{V}^\top\right) \\
&\quad + \epsilon\left(\mathbf{I} - \mathbf{U}\mathbf{U}^\top\right)\mathbf{W}\mathbf{V}\Sigma^{-1}\mathbf{V}^\top + \left(\mathbf{I} - \mathbf{U}\mathbf{U}^\top\right)\mathbf{W}\left(\mathbf{I} - \mathbf{V}\mathbf{V}^\top\right),
\end{aligned}$$

where the last equality shows the statement of Lemma 4.1.2. □

As a preparation for the proof of the last statement of Lemma 4.1, we formulate the following lemma which relates the gradient of F_ϵ at $\mathbf{W}$ with the reweighting operator.

Lemma A.4 (Gradient Condition)**.** *Let $\epsilon > 0$ For any $\mathbf{W} \in \mathbb{R}^{d_1 \times d_2}$, the reweighting operator $\mathcal{R}_{\mathbf{W},\epsilon} : \mathbb{R}^{d_1 \times d_2} \to \mathbb{R}^{d_1 \times d_2}$ satisfies*

$$\mathcal{R}_{\mathbf{W},\epsilon}(\mathbf{W}) = \nabla F_\epsilon(\mathbf{W}), \tag{12}$$

where $\nabla F_\epsilon(\mathbf{W})$ is the gradient of the ϵ-smoothed log-determinant at $\mathbf{W}$.

Proof. If $\mathbf{W} = \mathbf{U}_\mathbf{W} \operatorname{dg}(\sigma_i(\mathbf{W}))\mathbf{V}_\mathbf{W}^\top$ is a singular value decomposition of $\mathbf{W}$ with $\mathbf{U}_\mathbf{W} = [\mathbf{U} \quad \mathbf{U}_\perp] \in \mathbb{R}^{d_1 \times d_1}$ and $\mathbf{V}_\mathbf{W} = [\mathbf{V} \quad \mathbf{V}_\perp] \in \mathbb{R}^{d_2 \times d_2}$, we observe that

$$\begin{aligned}
\mathcal{R}_{\mathbf{W},\epsilon}(\mathbf{W}) &= \mathbf{U}_\mathbf{W}\Sigma_{\epsilon,d_1}^{-1}\mathbf{U}_\mathbf{W}^\top\left(\mathbf{U}_\mathbf{W}\operatorname{dg}(\sigma_i(\mathbf{W}))\mathbf{V}_\mathbf{W}^\top\right)\mathbf{V}_\mathbf{W}\Sigma_{\epsilon,d_2}^{-1}\mathbf{V}_\mathbf{W}^\top \\
&= \mathbf{U}_\mathbf{W}\Sigma_{\epsilon,d_1}^{-1}\operatorname{dg}(\sigma_i(\mathbf{W}))\Sigma_{\epsilon,d_2}^{-1}\mathbf{V}_\mathbf{W}^\top \\
&= \mathbf{U}_\mathbf{W}\operatorname{dg}\left(\frac{\sigma_i(\mathbf{W})}{\max(\sigma_i(\mathbf{W})/\epsilon, 1)^2}\right)_{i=1}^{d}\mathbf{V}_\mathbf{W}^\top = \nabla F_\epsilon(\mathbf{W}),
\end{aligned}$$

using the gradient formula Lemma A.2 in the last equality. □

As a corollary of Lemma A.4, we see that for $\mathbf{W}' = \mathbf{W}$, the gradient of the `Q3R` regularizer satisfies

$$\nabla \, \mathrm{Q3R}_{\mathbf{W},\epsilon}(\mathbf{W}) = \nabla F_\epsilon(\mathbf{W}).$$

This is this a direct implication of Lemma A.4 since

$$\nabla_{\mathbf{W}} \, \mathrm{Q3R}_{\mathbf{W}'=\mathbf{W},\epsilon}(\mathbf{W}) = \nabla_{\mathbf{W}} \left(\frac{1}{2} \langle \mathbf{W}, \mathcal{R}_{\mathbf{W}'=\mathbf{W},\epsilon}(\mathbf{W}) \rangle \right) = \mathcal{R}_{\mathbf{W},\epsilon}(\mathbf{W})$$

using the self-adjointness (see, e.g., (KM23, Appendix B)) of $\mathcal{R}_{\mathbf{W},\epsilon}$.

The gradient condition (12) enables us to equate the definition of the quadratic model function (2) $Q_\epsilon(\cdot \mid \mathbf{W}')$ (which is, up to a constant that depends on ϵ and $\mathbf{W}'$ the same as the value of `Q3R`) with the standard quadratic model form of (5).

Proof of Lemma 4.1.3. Let $\mathbf{W}, \mathbf{W}' \in \mathbb{R}^{d_1 \times d_2}$ be arbitrary. To show the equation (5), we start with its right hand side. By inserting (12), we obtain

$$\begin{aligned}
& F_\epsilon(\mathbf{W}') + \langle \nabla F_\epsilon(\mathbf{W}'), \mathbf{W} - \mathbf{W}' \rangle + \tfrac{1}{2} \langle \mathbf{W} - \mathbf{W}', \, \mathcal{R}_{\mathbf{W}',\epsilon}(\mathbf{W} - \mathbf{W}') \rangle \\
&= F_\epsilon(\mathbf{W}') + \langle \mathcal{R}_{\mathbf{W}',\epsilon}(\mathbf{W}'), \mathbf{W} - \mathbf{W}' \rangle + \frac{1}{2} \langle \mathbf{W}, \mathcal{R}_{\mathbf{W}',\epsilon}(\mathbf{W}) \rangle - \langle \mathcal{R}_{\mathbf{W}',\epsilon}(\mathbf{W}'), \mathbf{W} \rangle \\
&+ \frac{1}{2} \langle \mathbf{W}', \mathcal{R}_{\mathbf{W}',\epsilon}(\mathbf{W}') \rangle \\
&= F_\epsilon(\mathbf{W}') + \frac{1}{2} \langle \mathbf{W}, \mathcal{R}_{\mathbf{W}',\epsilon}(\mathbf{W}) \rangle - \frac{1}{2} \langle \mathbf{W}', \mathcal{R}_{\mathbf{W}',\epsilon}(\mathbf{W}') \rangle \\
&=: Q_\epsilon(\mathbf{W} \mid \mathbf{W}'),
\end{aligned}$$

where we also use the self-adjointness of $\mathcal{R}_{\mathbf{W}',\epsilon}(\cdot)$ in the first equality. The last expression corresponds to the definition of the quadratic model $Q_\epsilon(\cdot \mid \mathbf{W}')$ of $F_\epsilon(\cdot)$ given the expansion point $\mathbf{W}'$. This concludes the proof. □

From this proof, it becomes clear that the quadratic model $Q_\epsilon(\cdot \mid \mathbf{W}')$ is a pure quadratic model with vanishing linear term. This implies that, for example, $Q_\epsilon(-\mathbf{W} \mid \mathbf{W}') = Q_\epsilon(\mathbf{W} \mid \mathbf{W}')$ for all $\mathbf{W}$, which reflects the geometry of the smoothed log-determinant $F_\epsilon(\cdot)$ better than a mixed quadratic model function as it likewise satisfies $F_\epsilon(-\mathbf{W}) = F_\epsilon(\mathbf{W})$.

B Computation of `Q3R` value

In this section, we provide an implementable algorithm for evaluating the `Q3R` regularizer $\mathrm{Q3R}_{\mathbf{W}',\epsilon}(\mathbf{W})$ as defined in (6), defined in Algorithm 3 below.

We note that strictly speaking, evaluating $\mathrm{Q3R}_{\mathbf{W}',\epsilon}(\mathbf{W})$ is never necessary in a training scheme such as Adam`Q3R`; however, evaluating $\mathrm{Q3R}_{\mathbf{W}',\epsilon}(\mathbf{W})$ might be insightful to keep track of the extent of the regularization.

First, we decompose the reweighting operator image such that

$$\mathcal{R}_{\mathbf{W}',\epsilon}(\mathbf{W}) = T_1^\epsilon + T_2^\epsilon + T_3^\epsilon + T_4^\epsilon$$

with

$$\begin{aligned}
T_1^\epsilon &= \epsilon^2 \, \mathbf{U} \, \mathbf{\Sigma}^{-1} \mathbf{U}^\top \, \mathbf{W} \, \mathbf{V} \, \mathbf{\Sigma}^{-1} \mathbf{V}^\top, \\
T_2^\epsilon &= \epsilon \, \mathbf{U} \, \mathbf{\Sigma}^{-1} \mathbf{U}^\top \, \mathbf{W} \, (\mathbf{I} - \mathbf{V}\mathbf{V}^\top), \\
T_3^\epsilon &= \epsilon \, (\mathbf{I} - \mathbf{U}\mathbf{U}^\top) \, \mathbf{W} \, \mathbf{V} \, \mathbf{\Sigma}^{-1} \mathbf{V}^\top, \\
T_4^\epsilon &= (\mathbf{I} - \mathbf{U}\mathbf{U}^\top) \, \mathbf{W} \, (\mathbf{I} - \mathbf{V}\mathbf{V}^\top).
\end{aligned}$$

Defining

$$\begin{aligned}
I_1 &= \langle \mathbf{W}, \, T_1^\epsilon \rangle = \epsilon^2 \, \mathrm{tr}\big(\mathbf{W}^\top \mathbf{U} \, \mathbf{\Sigma}^{-1} \mathbf{U}^\top \mathbf{W} \, \mathbf{V} \, \mathbf{\Sigma}^{-1} \mathbf{V}^\top\big), \\
I_2 &= \langle \mathbf{W}, \, T_2^\epsilon \rangle = \epsilon \, \mathrm{tr}\big(\mathbf{W}^\top \mathbf{U} \, \mathbf{\Sigma}^{-1} \mathbf{U}^\top \mathbf{W} \, (\mathbf{I} - \mathbf{V}\mathbf{V}^\top)\big), \\
I_3 &= \langle \mathbf{W}, \, T_3^\epsilon \rangle = \epsilon \, \mathrm{tr}\big(\mathbf{W}^\top (\mathbf{I} - \mathbf{U}\mathbf{U}^\top) \, \mathbf{W} \, \mathbf{V} \, \mathbf{\Sigma}^{-1} \mathbf{V}^\top\big), \\
I_4 &= \langle \mathbf{W}, \, T_4^\epsilon \rangle = \mathrm{tr}\big(\mathbf{W}^\top (\mathbf{I} - \mathbf{U}\mathbf{U}^\top) \, \mathbf{W} \, (\mathbf{I} - \mathbf{V}\mathbf{V}^\top)\big),
\end{aligned}$$

we can write

$$\big\langle \mathbf{W}, \mathcal{R}_{\mathbf{W}',\epsilon}(\mathbf{W}) \big\rangle = I_1 + I_2 + I_3 + I_4.$$

Apply cyclicity to I_1, I_2, I_3.

$$\begin{aligned}
I_1 &= \epsilon^2 \operatorname{tr}\big(\mathbf{V}^\top \mathbf{W}^\top \mathbf{U}\,\mathbf{\Sigma}^{-1}\mathbf{U}^\top \mathbf{W}\,\mathbf{V}\,\mathbf{\Sigma}^{-1}\big),\\
I_2 &= \epsilon \Big[\operatorname{tr}\big(\mathbf{W}^\top \mathbf{U}\,\mathbf{\Sigma}^{-1}\mathbf{U}^\top \mathbf{W}\big) \;-\; \operatorname{tr}\big(\mathbf{W}^\top \mathbf{U}\,\mathbf{\Sigma}^{-1}\mathbf{U}^\top \mathbf{W}\,\mathbf{V}\mathbf{V}^\top\big)\Big],\\
I_3 &= \epsilon \Big[\operatorname{tr}\big(\mathbf{W}^\top \mathbf{W}\,\mathbf{V}\,\mathbf{\Sigma}^{-1}\mathbf{V}^\top\big) \;-\; \operatorname{tr}\big(\mathbf{W}^\top \mathbf{U}\mathbf{U}^\top \mathbf{W}\,\mathbf{V}\,\mathbf{\Sigma}^{-1}\mathbf{V}^\top\big)\Big].
\end{aligned}$$

Expand I_4.

$$I_4 = \operatorname{tr}\big(\mathbf{W}^\top \mathbf{W}\big) \;-\; \operatorname{tr}\big(\mathbf{W}^\top \mathbf{W}\,\mathbf{V}\,\mathbf{V}^\top\big) \;-\; \operatorname{tr}\big(\mathbf{W}^\top \mathbf{U}\mathbf{U}^\top \mathbf{W}\big) \;+\; \operatorname{tr}\big(\mathbf{W}^\top \mathbf{U}\mathbf{U}^\top \mathbf{W}\,\mathbf{V}\,\mathbf{V}^\top\big).$$

Group terms.

$$\begin{aligned}
\big\langle \mathbf{W}, \mathcal{R}_{\mathbf{W}',\epsilon}(\mathbf{W}) \big\rangle = {} & \operatorname{tr}(\mathbf{W}^\top \mathbf{W})\\
& + \epsilon^2 \operatorname{tr}\big(\mathbf{V}^\top \mathbf{W}^\top \mathbf{U}\,\mathbf{\Sigma}^{-1}\mathbf{U}^\top \mathbf{W}\,\mathbf{V}\,\mathbf{\Sigma}^{-1}\big)\\
& + \epsilon \operatorname{tr}\big(\mathbf{W}^\top \mathbf{U}\,\mathbf{\Sigma}^{-1}\mathbf{U}^\top \mathbf{W}\big) \;-\; \epsilon \operatorname{tr}\big(\mathbf{W}^\top \mathbf{U}\,\mathbf{\Sigma}^{-1}\mathbf{U}^\top \mathbf{W}\,\mathbf{V}\mathbf{V}^\top\big)\\
& + \epsilon \operatorname{tr}\big(\mathbf{W}^\top \mathbf{W}\,\mathbf{V}\,\mathbf{\Sigma}^{-1}\mathbf{V}^\top\big) \;-\; \epsilon \operatorname{tr}\big(\mathbf{W}^\top \mathbf{U}\mathbf{U}^\top \mathbf{W}\,\mathbf{V}\,\mathbf{\Sigma}^{-1}\mathbf{V}^\top\big)\\
& - \operatorname{tr}\big(\mathbf{W}^\top \mathbf{W}\,\mathbf{V}\,\mathbf{V}^\top\big) \;-\; \operatorname{tr}\big(\mathbf{W}^\top \mathbf{U}\mathbf{U}^\top \mathbf{W}\big) \;+\; \operatorname{tr}\big(\mathbf{W}^\top \mathbf{U}\mathbf{U}^\top \mathbf{W}\,\mathbf{V}\,\mathbf{V}^\top\big).
\end{aligned}$$

Then by rearranging each pair of trace-terms we arrive at

$$\begin{aligned}
\big\langle \mathbf{W}, \mathcal{R}_{\mathbf{W}',\epsilon}(\mathbf{W}) \big\rangle = {} & \operatorname{tr}\big(\mathbf{W}^\top \mathbf{W}\big)\\
& + \operatorname{tr}\big(\mathbf{U}^\top \mathbf{W}\,\mathbf{W}^\top \mathbf{U}\,(\epsilon\,\mathbf{\Sigma}^{-1} - \mathbf{I})\big)\\
& + \operatorname{tr}\big(\mathbf{V}^\top \mathbf{W}^\top \mathbf{W}\,\mathbf{V}\,(\epsilon\,\mathbf{\Sigma}^{-1} - \mathbf{I})\big)\\
& + \operatorname{tr}\big(\mathbf{V}^\top \mathbf{W}^\top \mathbf{U}\,(\epsilon\,\mathbf{\Sigma}^{-1} - \mathbf{I})\,\mathbf{U}^\top \mathbf{W}\,\mathbf{V}\,(\epsilon\,\mathbf{\Sigma}^{-1} - \mathbf{I})\big).
\end{aligned}$$

For each iteration we calculate the quadratic regularizer $\langle \mathbf{W}, \mathcal{R}_{\mathbf{W}',\epsilon}(\mathbf{W})\rangle$ for weight matrices $\mathbf{W}$. For algorithmic simplicity, We now re-arrange the summand of our `Q3R` regularizer and show the simplified expression for this inner product in Algorithm 3. We later show in Equation (13), where we derive the expression of this inner product and we show that this matches the one proposed in Algorithm 3.

$$\begin{aligned}
& f = \underbrace{\operatorname{tr}\big(\mathbf{W}^\top \mathbf{W}\big)}_{t_1} + \underbrace{\operatorname{tr}\big(\mathbf{V}^\top \mathbf{W}^\top \mathbf{U}\,\mathbf{S}\,\mathbf{U}^\top \mathbf{W}\,\mathbf{V}\,\mathbf{S}\big)}_{t_2} + \underbrace{\operatorname{tr}\big(\mathbf{V}^\top \mathbf{W}^\top \mathbf{W}\,\mathbf{V}\,\mathbf{S}\big)}_{t_3} + \underbrace{\operatorname{tr}\big(\mathbf{U}^\top \mathbf{W}\,\mathbf{W}^\top \mathbf{U}\,\mathbf{S}\big)}_{t_4},\\
& \mathbf{S} = \epsilon\,\mathbf{\Sigma}^{-1} - \mathbf{I},\\
& \mathbf{T} = \mathbf{W}\,\mathbf{V}, \quad \mathbf{B} = \mathbf{W}^\top \mathbf{U}, \quad \mathbf{C} = \mathbf{U}^\top \mathbf{W}\,\mathbf{V}, \quad \mathbf{M} = \mathbf{S}^{1/2}\,\mathbf{C}\,\mathbf{S}^{1/2}.
\end{aligned}$$

Using $\operatorname{tr}(\mathbf{A}^\top \mathbf{A}) = \|\mathbf{A}\|_F^2$ and cyclicity:

$$\begin{aligned}
t_1 &= \operatorname{tr}(\mathbf{W}^\top \mathbf{W}) = \|\mathbf{W}\|_F^2,\\
t_2 &= \operatorname{tr}\big(\mathbf{S}\,(\mathbf{U}^\top \mathbf{W}\mathbf{V})\,\mathbf{S}\,(\mathbf{U}^\top \mathbf{W}\mathbf{V})\big) = \|\mathbf{M}\|_F^2,\\
t_3 &= \operatorname{tr}\big(\mathbf{S}\,(\mathbf{W}\mathbf{V})^\top (\mathbf{W}\mathbf{V})\big) = \|\mathbf{T}\,\mathbf{S}^{1/2}\|_F^2,\\
t_4 &= \operatorname{tr}\big(\mathbf{S}\,(\mathbf{W}^\top \mathbf{U})^\top (\mathbf{W}^\top \mathbf{U})\big) = \|\mathbf{B}\,\mathbf{S}^{1/2}\|_F^2.
\end{aligned}$$

Putting it all together, with $\mathbf{R} = \mathbf{S}^{1/2}$:

$$f(\mathbf{W}, \mathbf{U}, \mathbf{V}) = \|\mathbf{W}\|_F^2 + \|\mathbf{M}\|_F^2 + \|\mathbf{T}\,\mathbf{R}\|_F^2 + \|\mathbf{B}\,\mathbf{R}\|_F^2, \qquad \mathbf{R} = (\epsilon\,\mathbf{\Sigma}^{-1} - \mathbf{I})^{1/2}. \tag{13}$$

Algorithm 3 Computation of the `Q3R` function value $\mathrm{Q3R}_{\mathbf{W}',\epsilon}(\mathbf{W})$

Input: $W \in \mathbb{R}^{d_1 \times d_2}$, $U \in \mathbb{R}^{d_1 \times r}$, $V \in \mathbb{R}^{d_2 \times r}$, $S \in \mathbb{R}^{r \times r}$
Output:e $f(W, U, V, S) = \|W\|_F^2 + \|\,M\|_F^2 + \|\,T\,R\|_F^2 + \|\,B\,R\|_F^2$
1. Compute projections
$T \leftarrow W\,V$ $\quad O(d_1 d_2 r)$
$B \leftarrow W^\top U$ $\quad O(d_1 d_2 r)$
2. Form intermediate products
$C \leftarrow U^\top T$ $\quad O(d_1 r^2)$
Compute symmetric square-root R of S: $R\,R^\top = S$ $\quad O(r^3)$
$M \leftarrow R\,C\,R^\top$ $\quad O(r^3)$
3. Evaluate Frobenius norms
$t_1 \leftarrow \|W\|_F^2$ $\quad O(d_1 d_2)$
$t_2 \leftarrow \|M\|_F^2$ $\quad O(r^2)$
$t_3 \leftarrow \|T\,R\|_F^2$ $\quad O(d_1 r^2 + d_1 r)$
$t_4 \leftarrow \|B\,R\|_F^2$ $\quad O(d_2 r^2 + d_2 r)$
return $f \leftarrow t_1 + t_2 + t_3 + t_4$

To summarize, we obtain a total FLOP count of

$$\boxed{T_{\text{total}} = 2\,d_1 d_2 r \;+\; (d_1 + d_2) r^2 \;+\; 2r^3 \;+\; \big(d_1 d_2 + (d_1 + d_2) r + r^2\big) = O\big(d_1 d_2 r \;+\; (d_1 + d_2) r^2 \;+\; r^3\big)}$$

for evaluating $\mathrm{Q3R}_{\mathbf{W}',\epsilon}(\mathbf{W})$.

C Computation of the Gradient of `Q3R`

From Equation (4), we rearrange the summand for algorithmic simplicity

$$\begin{aligned}\mathcal{R}_{\mathbf{W}',\epsilon}(\mathbf{W}) &= \epsilon^2\,\mathbf{U}\,\mathbf{\Sigma}^{-1}\mathbf{U}^\top\,\mathbf{W}\,\mathbf{V}\,\mathbf{\Sigma}^{-1}\mathbf{V}^\top \;+\; \epsilon\,\mathbf{U}\,\mathbf{\Sigma}^{-1}\mathbf{U}^\top\,\mathbf{W}\,(\mathbf{I} - \mathbf{V}\mathbf{V}^\top) \\ &\quad +\; \epsilon\,(\mathbf{I} - \mathbf{U}\mathbf{U}^\top)\,\mathbf{W}\,\mathbf{V}\,\mathbf{\Sigma}^{-1}\mathbf{V}^\top \;+\; (\mathbf{I} - \mathbf{U}\mathbf{U}^\top)\,\mathbf{W}\,(\mathbf{I} - \mathbf{V}\mathbf{V}^\top).\end{aligned}$$

Using $\epsilon\,\mathbf{\Sigma}^{-1} = \mathbf{I} + \mathbf{S}$, we rewrite each term:

$$\begin{aligned}T_1^\epsilon &= \epsilon^2\,\mathbf{U}\,\mathbf{\Sigma}^{-1}\mathbf{U}^\top\,\mathbf{W}\,\mathbf{V}\,\mathbf{\Sigma}^{-1}\mathbf{V}^\top = \mathbf{U}\,(\mathbf{I} + \mathbf{S})\,\mathbf{U}^\top\,\mathbf{W}\,\mathbf{V}\,(\mathbf{I} + \mathbf{S})\,\mathbf{V}^\top, \\ T_2^\epsilon &= \epsilon\,\mathbf{U}\,\mathbf{\Sigma}^{-1}\mathbf{U}^\top\,\mathbf{W}\,(\mathbf{I} - \mathbf{V}\mathbf{V}^\top) = \mathbf{U}\,(\mathbf{I} + \mathbf{S})\,\mathbf{U}^\top\,\mathbf{W}\,(\mathbf{I} - \mathbf{V}\mathbf{V}^\top), \\ T_3^\epsilon &= \epsilon\,(\mathbf{I} - \mathbf{U}\mathbf{U}^\top)\,\mathbf{W}\,\mathbf{V}\,\mathbf{\Sigma}^{-1}\mathbf{V}^\top = (\mathbf{I} - \mathbf{U}\mathbf{U}^\top)\,\mathbf{W}\,\mathbf{V}\,(\mathbf{I} + \mathbf{S})\,\mathbf{V}^\top, \\ T_4^\epsilon &= (\mathbf{I} - \mathbf{U}\mathbf{U}^\top)\,\mathbf{W}\,(\mathbf{I} - \mathbf{V}\mathbf{V}^\top).\end{aligned}$$

Collecting like-terms in powers of $\mathbf{S}$ gives the compact form

$$\boxed{\mathcal{R}_{\mathbf{W}',\epsilon}(\mathbf{W}) = \underbrace{\mathbf{W}}_{T_1} + \underbrace{\mathbf{U}\,\mathbf{S}\,\mathbf{U}^\top\,\mathbf{W}}_{T_2} + \underbrace{\mathbf{W}\,\mathbf{V}\,\mathbf{S}\,\mathbf{V}^\top}_{T_3} + \underbrace{\mathbf{U}\,\mathbf{S}\,\mathbf{U}^\top\,\mathbf{W}\,\mathbf{V}\,\mathbf{S}\,\mathbf{V}^\top}_{T_4}}$$

with $\mathbf{S} = \epsilon\,\mathbf{\Sigma}^{-1} - \mathbf{I}$.

Now, we deduce the gradient in the following algorithm that is used in line 12 of Algorithm 2. We explain the step-by-step computation of our $R_{\mathbf{W}',\epsilon}(\mathbf{W})$ stated below.

Algorithm 4 COMPUTATION GRADIENT OF `Q3R` : Compute $\mathcal{R}_{\mathbf{W}',\epsilon}(\mathbf{W})$

Input: $\mathbf{W} \in \mathbb{R}^{d_1 \times d_2}$, $\mathbf{U} \in \mathbb{R}^{d_1 \times r}$, $\mathbf{V} \in \mathbb{R}^{d_2 \times r}$, singular values $\boldsymbol{\sigma} \in \mathbb{R}^{r}_{>0}$, threshold ϵ
Output: $\mathbf{G} = \mathcal{R}_{\mathbf{W}',\epsilon}(\mathbf{W})$

$s \leftarrow 1/\max(\boldsymbol{\sigma},\ 1)$ ▷ r element-wise comparisons
$S \leftarrow \mathrm{diag}(s)$ ▷ create diagonal matrix of shape $r \times r$
$S_{\text{shift}} \leftarrow \epsilon S - I$ ▷ r subtractions on diagonal

$A \leftarrow \mathbf{U}^\top \mathbf{W}$ ▷ $r \times d_1$ by $d_1 \times d_2 \to r \times d_2$ (cost: rd_1d_2)
$B \leftarrow \mathbf{W}\,\mathbf{V}$ ▷ $d_1 \times d_2$ by $d_2 \times r \to d_1 \times r$ (cost: d_1d_2r)

$C \leftarrow A \cdot \mathbf{V}$ ▷ $r \times d_2$ by $d_2 \times r \to r \times r$ (cost: rd_2r)
$E \leftarrow S_{\text{shift}} \cdot C \cdot S_{\text{shift}}$ ▷ $r \times r$ triple product (cost: $2r^3$)
for $i = 1, \ldots, r$ **do**
  for $j = 1, \ldots, r$ **do**
    $E_{ij} \leftarrow (S_{\text{shift}})_{ii} \cdot C_{ij} \cdot (S_{\text{shift}})_{jj}$
end for end for ▷ elementwise scalar products (cost: r^2)
$T_2 \leftarrow \mathbf{U} \cdot E \cdot \mathbf{V}^\top$ ▷
- $\mathbf{U} \cdot E$: $d_1 \times r$ by $r \times r \to d_1 \times r$ (cost: d_1r^2)
- Then $\cdot\mathbf{V}^\top$: $d_1 \times r$ by $r \times d_2 \to d_1 \times d_2$ (cost: d_1d_2r)

$T_1 \leftarrow \mathbf{W}$ ▷ copy or identity operation ($d_1 \times d_2$)
$T_3 \leftarrow B \cdot S_{\text{shift}} \cdot \mathbf{V}^\top$ ▷
- $B \cdot S_{\text{shift}}$: $d_1 \times r$ by $r \times r \to d_1 \times r$ (cost: d_1r^2)
- Then $\cdot\mathbf{V}^\top$: $d_1 \times r$ by $r \times d_2 \to d_1 \times d_2$ (cost: d_1d_2r)

$D \leftarrow S_{\text{shift}} \cdot A$ ▷ $r \times r$ by $r \times d_2 \to r \times d_2$ (cost: r^2d_2)
$T_4 \leftarrow \mathbf{U} \cdot D$ ▷ $d_1 \times r$ by $r \times d_2 \to d_1 \times d_2$ (cost: d_1rd_2)

gradient $\leftarrow T_1 + T_2 + T_3 + T_4$ ▷ elementwise addition of $d_1 \times d_2$ matrices
return gradient

D Experimental Results

In this section, we provide details regarding the experimental training methodology of Section 5 as well as some additional data of these experiments.

D.1 Experimental Protocol

In the experiments, we compared the training of unregularized models, as well as models regularized by `Q3R` , LoRITa (AZW) and LoRA (HSW+22a). Due to the limitations of some techniques not providing strong truncation guide lines, we truncate each method at various truncation ranks r. Ensuring such that r is chosen to always ensure that the factor matrix pairs always have less original parameters, to minimize a practical environment. In Table 1 we find that running with $p = .20$ or $r = 19$ and $\lambda = 0.001$ performs best given the truncation and accuracy trade-offs.

ViT Hyperparameter Selection We selected each model's learning rate based on the performance of the unmodified ViT model for each respective dataset. All ViT models were configured with an input resolution of 224×224 pixels and utilized patch size 16 for tokenization. LoRITa hyperparameter optimization was conducted through grid search with regularization parameter $\lambda \in \{10^{-1}, 10^{-2}, 10^{-3}, 10^{-4}\}$ and rank parameter $d \in \{1, 2, 3\}$ to ensure optimal performance. The best-performing configuration from three independent runs was selected for evaluation across additional datasets. LoRA was evaluated across various target ranks, with the proportion parameter p selected from $p \in \{0.05, 0.15, 0.3, 0.4, 0.5, 0.6, 0.7, 0.8, 0.9\}$. AdamQ3R underwent grid search optimization with regularization parameter $\lambda \in \{10^{-3}, 10^{-2}, 10^{-1}\}$ and proportion parameter $r \in \{0.05, 0.1, 0.15, 0.2\}$, with a stable $period = 5$. The regularization strength remained constant regardless of matrix dimensions. The QKV projection matrices were selected as the target for modification due to their prevalence in the literature as candidates for model compression and adaptation.

CIFAR-100 Data Augmentation For CIFAR-100 experiments, we applied comprehensive data augmentation during training, including random cropping with 4-pixel padding from the original 32×32 images, random horizontal flipping, and subsequent resizing to 224×224 pixels to match the ViT input requirements. Images were normalized using channel-wise means of (0.4914, 0.4822, 0.4465) and standard deviations of (0.2023, 0.1994, 0.2010), corresponding to the CIFAR-100 dataset statistics. The test set underwent only resizing to 224×224 pixels and the same normalization procedure, without augmentation.

Fine-Tuning Experimental Details We fine-tuned the pre-trained RoBERTa-Base model (from Hugging Face) on all nine GLUE tasks using a maximum sequence length of 512 and a batch size of 16 (30 for CoLA). We run all fine-tuning experiments with a target rank as low as 4. The best performing setup had 'reweighting period' of 3 and $\lambda \in \{1.5, 2\}$. As shown in Table 3, we compare `Q3R` with LoRA and dense fine-tuning. The tasks and their metrics are summarized below:

- **Single-Sentence Classification**
  - CoLA: 8.5 k train / 1 k test; linguistic acceptability; Matthews correlation
  - SST-2: 67 k train / 1.8 k test; sentiment classification; accuracy
- **Similarity & Paraphrase**
  - MRPC: 3.7 k train / 1.7 k test; paraphrase detection; accuracy / F1
  - STS-B: 7 k train / 1.4 k test; sentence similarity; Pearson / Spearman correlation
  - QQP: 364 k train / 391 k test; question paraphrase detection; accuracy / F1
- **Natural Language Inference**
  - MNLI: 393 k train / 20 k matched + 20 k mismatched test; entailment classification; accuracy
  - QNLI: 105 k train / 5.4 k test; question–answer entailment; accuracy
  - RTE: 2.5 k train / 3 k test; textual entailment; accuracy
  - WNLI: 634 train / 146 test; coreference-based inference; accuracy

D.2 Fine-tuning Experiments

To assess the potential of `Q3R` for fine-tuning large language models, we conducted an additional experiment on Llama 3.2–3B using an NVIDIA A5000 GPU. Since the original `meta-llama/Llama-3.2-3B` checkpoint provides only the pre-trained language model parameters, we instantiated the `LlamaForSequenceClassification` module, which attaches an additional linear projection, commonly referred to as the *classification head*, on top of the final hidden-state representation. This head, whose weight matrix is registered as `score.weight` (and optionally `score.bias`), is absent from the checkpoint and was therefore initialized with random Gaussian values.

The fine-tuning setup involves training this weight matrix as well as additive weights for the Q, K, and V layers.

With `Q3R` ($\lambda = 0.0001$, target rank $= 4$, for 100 epochs), we achieved an F1 score of 81.89% on the MRPC dataset of the GLUE benchmark, whereas full fine-tuning (effectively corresponding to setting $\lambda = 0$) resulted in an F1 score of 80.7% after the same number of epochs.

To further compare our proposed method, we conducted experiemnts on Llama3.2-1B on a subset of the GLUE tasks. Table 4 provides a comparison of our method's performance with dense fine-tuning and LoRA.

We achieved the performance as mentioned in Table 4, with a single value of λ without any extensive hyperparameter search. While we acknowledge that better performance for GLUE tasks like RTE can often be obtained by starting from a more finely tuned initialization, these results demonstrate that the proposed method is effective even for the fine-tuning of large-scale LLMs.

Table 4: GLUE Benchmark Results for Llama3.2-1B

Model	**MRPC**	**SST-2**	**RTE**	**CoLA**	**STS-B**
Dense	86.3	95.3	77.3	47.09	90.5
LoRA rank=4	87.3	95.7	80.9	61.8	89.1
Q3R rank=4	87.8	94.4	64.7	51.8	87.04

D.3 Appendix Tables

Table 5 and Table 6 demonstrate the low rank induction techniques on ViT models. We train ViT-B on CIFAR-100 in Table 6 and ViT-T on CIFAR-10 in Table 5 respectively.

Table 5: Performance at varying percentages of parameters saved on ViT-T when regularizer is applied to only attention blocks.

Model	**15%**	**20%**	**30%**	**40%**	**50%**	**60%**	**70%**	**80%**	**90%**	**100%**
Vanilla ViT-T	0.4687	0.5430	0.5892	0.6170	0.6542	0.6694	0.6726	0.6788	0.6892	0.7027
Q3R rank=4, λ=0.01	0.6032	0.6630	0.7043	0.7060	0.7084	0.7080	0.7079	0.7079	0.7077	0.7152
Q3R rank=9, λ=0.01	0.4852	0.5616	0.6668	0.6772	0.6831	0.6835	0.6832	0.6829	0.6831	0.7034
Q3R rank=14, λ=0.01	0.4576	0.5812	0.6866	0.6970	0.6988	0.7002	0.6997	0.6996	0.7003	0.7104
Q3R rank=19, λ=0.01	0.6208	0.6792	0.6913	0.6977	0.6978	0.6970	0.6970	0.6967	0.6966	0.7061
Q3R rank=4, λ=0.001	0.5694	0.6629	0.7017	0.7053	0.7084	0.7091	0.7086	0.7086	0.7079	0.7158
Q3R rank=9, λ=0.001	0.4214	0.5304	0.6467	0.6680	0.6691	0.6692	0.6691	0.6696	0.6695	0.6955
Q3R rank=14, λ=0.001	0.6040	0.6364	0.6642	0.6695	0.6695	0.6694	0.6698	0.6701	0.6704	0.6819
LoRITa D=1, α=0.1	0.1154	0.1217	0.1234	0.1091	0.1502	0.2310	0.3377	0.4197	0.5027	0.7061
LoRITa D=1, α=0.001	0.1576	0.1512	0.1602	0.1586	0.1902	0.2456	0.2955	0.3221	0.4056	0.7086
LoRITa D=1, α=0.01	0.1474	0.1514	0.1539	0.1644	0.2486	0.2968	0.4150	0.4857	0.5326	0.6911
LoRITa D=2, α=0.01	0.2478	0.2559	0.3115	0.4065	0.5127	0.5641	0.5997	0.6456	0.6720	0.7287
LoRITa D=2, α=0.1	0.2041	0.2589	0.3639	0.5397	0.5982	0.6408	0.6727	0.6910	0.7025	0.7595
LoRITa D=2, α=0.001	0.2195	0.2774	0.4163	0.5115	0.5461	0.5675	0.6137	0.6417	0.6614	0.7393
LoRITa D=3, α=0.01	0.3794	0.5074	0.5907	0.6385	0.6598	0.6761	0.6843	0.6916	0.6959	0.7462
LoRITa D=3, α=0.001	0.3951	0.5147	0.5952	0.6308	0.6639	0.6676	0.6798	0.6847	0.6833	0.7367
LoRA rank=4	0.3443	0.3443	0.3443	0.3443	0.3443	0.3443	0.3443	0.3443	0.3443	0.3443
LoRA rank=14	0.5859	0.5859	0.5859	0.5859	0.5859	0.5859	0.5859	0.5859	0.5859	0.5859

Table 6: CIFAR-100 Performance with ViT-B Attention Block Truncation

Model	**5%**	**10%**	**15%**	**20%**	**30%**	**40%**	**100%**
Vanilla ViT-B Best	0.2773	0.3355	0.3659	0.3909	0.4172	0.4327	**0.4686**
Q3R, rank=19, λ=0.01	0.3238	**0.3979**	**0.4172**	**0.4301**	**0.4411**	**0.4485**	0.4625
Q3R, rank=19, λ=0.001	0.3174	0.3790	0.3945	0.4050	0.4130	0.4197	0.4408
Q3R, rank=14, λ=0.001	0.3250	0.3978	0.4149	0.4240	0.4351	0.4429	0.4613
Q3R, rank=14, λ=0.01	**0.3465**	0.3950	0.4062	0.4172	0.4305	0.4389	0.4526
LoRITa D=2, α=0.1	0.0152	0.0444	0.0883	0.1404	0.2428	0.3043	0.4021
LoRITa D=3, α=0.001	0.0607	0.1375	0.2001	0.2380	0.2975	0.3269	0.4103
LoRITa D=3, α=0.1	0.0570	0.1369	0.2003	0.2401	0.2946	0.3188	0.4111

D.4 Computational Aspects

For few experiments like `Q3R`, we used NVIDIA A5000 to train the ViT models. The rest of the experiments were performed on NVIDIA V100 with 32GB memory. The fine-tuning experiemtns were all performed in NVIDIA A5000 GPUs.

D.5 Computational Overhead of Methodology

In Algorithms 3 and 4, we provide the detailed stepwise FLOP count of our method. Following the experiments testing the influence of the reweighting period on the truncation, we report the average training time of the first 5 epochs below. Note that regularization was only applied on the QKV matrices of a ViT-Tiny Transformer.

Table 7: Average training time (5 epochs) and reserved GPU memory for ViT-Tiny with QKV-only regularization.

Model	Variant / Setting	Avg. Time (s)	Reserved GPU Mem (GB)
Base	—	150.91	6.26
AdamQ3R	T=500	205.34	6.28
	T=100	207.39	6.31
	T=50	209.29	6.62
	T=20	217.90	8.22
	T=10	218.88	8.62
LoRA	R=4	124.83	11.89
	R=14	144.51	11.87
	R=28	145.28	11.89
Depth1 baseline	—	157.29	8.35

Based on the theoretical computational overhead outlined in Algorithm 3 Algorithm 1, along with the results above, we expect `Q3R` to incur additional computational and memory overhead. The added memory originates from the additional weight matrices stored in `Q3R` to perform the weight least squares minimization. We attribute the lower Reserved GPU Memory from implementation differences in the optimizer.

E Ablation Studies

Table 8 presents the comparison between the regularization term (6) and Algorithm 2 evaluated across varied truncation levels and hyperparameters. Initially AdamQ3R presents competitive performance against `Q3R`; however, `Q3R` provides superior truncation performance on the validation set at lower truncation values (20% and below). The impact of the regularization parameter is notably small, with $\lambda = 0.001$ generally providing superior performance.

Table 8: Performance of Vit-T with AdamQ3R and `Q3R` across different truncation level on CIFAR10.

Model Name	5%	10%	15%	20%	30%	40%	100%
AdamQ3R, rank = 0.05*	0.1904	0.4600	0.6032	0.6630	0.7043	0.7060	0.7152
AdamQ3R, rank = 0.10*	0.2081	0.3591	0.4852	0.5616	0.6668	0.6772	0.7034
AdamQ3R, rank = 0.15*	0.1266	0.3970	0.4576	0.5812	0.6866	0.6970	0.7104
AdamQ3R, rank = 0.20*	0.1740	0.4717	0.6208	0.6792	0.6913	0.6977	0.7061
AdamQ3R, rank = 0.05^	0.2701	0.4608	0.5694	0.6629	0.7017	0.7053	**0.7158**
AdamQ3R, rank = 0.10^	0.1066	0.1741	0.4214	0.5304	0.6467	0.6680	0.6955
AdamQ3R, rank = 0.15^	0.2467	0.4993	0.6040	0.6364	0.6642	0.6695	0.6819
Q3R, rank = 0.04*	0.2476	0.5171	0.6544	0.6862	0.6884	0.6874	0.6920
Q3R, rank = 0.09*	0.1959	0.5040	0.6789	0.6789	0.6862	0.6870	0.6827
Q3R, rank = 0.19*	0.2774	0.4317	0.6337	0.6697	0.6818	0.6896	0.6901
Q3R, rank = 0.04^	0.2828	0.4699	0.6004	0.6569	0.6801	0.6801	0.6934
Q3R, rank = 0.09^	**0.3202**	**0.5527**	**0.6827**	**0.7024**	**0.7024**	**0.7079**	0.7081
Q3R, rank = 0.19^	0.3119	0.4440	0.6137	0.6670	0.6839	0.6877	0.6885

Legend: * Regularization parameter $\lambda = 0.01$, ^ Regularization parameter $\lambda = 0.001$

E.1 Robustness to Hyperparameter Variations

Empirically, we found Q3R to be quite robust to its hyperparameters within reasonable ranges. Below, we are providing few empirical evidences from Table 1on ViT-Tiny. However, similar results can be conducted across other datasets and backbones as in Table 4 (CIFAR-100 on ViT-Base). Generally, when choosing λ, a viable rule is easy to tell if the choice of lambda is too small by monitoring if the Q3R value increases within the first few epochs. We recommend a value of λ that is slightly larger than the lower bound of the divergence threshold, as determining if the λ value is too large remains a challenge.

Table 9: Effect of regularization strength λ on accuracy.

Parameter Retention	**Accuracy (%)**
1%	46.08–46.30
5%	63.40–63.65
10%	66.30–66.40
25%	70.68–70.74
50%	71.04–71.09
100% (no trunc.)	71.95–71.52

Beyond the 20% retention point, the absolute accuracy gap never exceeds 0.3 percentage points, confirming that AdamQ3R is largely insensitive to λ within the 0.001–0.01 range in this practical operating regime.

Table 10: Effect of target rank r_{target} on accuracy.

Retention (%)	**Accuracy (%)**
1%	0.5683
5%	0.6568
10%	0.7068
25%	0.6671
50%	0.6457
100%	0.6663

Once 30% of the parameters are retained, the choice of rank changes accuracy by $< 0.3\%$, confirming low sensitivity to rank in this regime. We here scale the target rank by layer dimensions so that a single hyper-parameter r works for networks of any size.

E.2 Merits of Low-Rank Initialization

In our experiments, we implemented supervised initialization where the regulated weight matrix has a rank greater than or equal to the target rank hyperparameter specified in Q3R. Our findings support the hypothesis that low-rank initialization in Q3R imposes a strong constraint on the optimization landscape when the rank is low, thereby limiting the model's capacity to explore more expensive solutions during training. This hypothesis is further supported by the fine-tuning results on RoBERTa where Q3R is applied to the pretrained model and continuously tuned on the GLUE benchmark tasks. We achieve notable results that support the general intuition that models tend to learn better representation through expensive subspaces during the training process. Due to the time constraint of the evaluation period, we could experiment on only the smaller data we observe that LowRank initialization is unable to surpass the performance of Q3R without such constraint on the initialization. However, the accuracy is within 1 range of the full rank initialized model which proves that our proposed method can be implemented in resource constrained setups as well. We provide the example of the empirical evidence performed on CIFAR-10 on ViT-Tiny with $\lambda = 0.05$ and $\alpha = 0.01$.

E.3 Choice of Reweighting Period

We observe in Table 12 that higher reweighting periods (T) (300, 200, 100) result in underperformance in comparison to the lower reweighting periods(T) (25, 5). While longer reweighting periods provide some computational performance gains based upon formulation Algorithm 1, we observe superior performance for faster intervals which corresponds to the IRLS-majorisation of the logdet.

Code : The code is available at `https://github.com/ThatE10/q3r.git`.

Table 11: Parameter retention effect on accuracy (AdamQ3R + LowRank).

Parameter Retention	Accuracy (%)
1%	46.08
5%	63.40
10%	66.30
25%	70.68
50%	71.04
100% (no trunc.)	72.19

Table 12: Model performance under different truncation percentages. Best value per column is bolded. Each model trained with $\lambda = 0.001, r = 0.2$, Trained for 30 epochs

Model Name	5%	10%	15%	20%	30%	40%	100%
AdamQ3R,T = 300	0.2999	0.5609	0.6651	0.6801	0.6847	0.6838	0.6827
AdamQ3R, T = 200	0.2601	0.5914	0.6519	0.6766	0.6869	0.6885	0.6871
AdamQ3R, T = 100	0.2764	0.4871	0.6623	0.6776	0.6869	0.6885	0.6936
AdamQ3R, T = 25	**0.3729**	0.5813	0.6555	0.6725	0.6734	0.6778	0.6790
AdamQ3R, T = 5	0.1740	**0.6838**	**0.6828**	**0.6949**	**0.6995**	**0.7000**	**0.7031**

NeurIPS Paper Checklist

The checklist is designed to encourage best practices for responsible machine learning research, addressing issues of reproducibility, transparency, research ethics, and societal impact. Do not remove the checklist: **The papers not including the checklist will be desk rejected.** The checklist should follow the references and follow the (optional) supplemental material. The checklist does NOT count towards the page limit.

Please read the checklist guidelines carefully for information on how to answer these questions. For each question in the checklist:

- You should answer [Yes] , [No] , or [NA] .
- [NA] means either that the question is Not Applicable for that particular paper or the relevant information is Not Available.
- Please provide a short (1–2 sentence) justification right after your answer (even for NA).

The checklist answers are an integral part of your paper submission. They are visible to the reviewers, area chairs, senior area chairs, and ethics reviewers. You will be asked to also include it (after eventual revisions) with the final version of your paper, and its final version will be published with the paper.

The reviewers of your paper will be asked to use the checklist as one of the factors in their evaluation. While "[Yes] " is generally preferable to "[No] ", it is perfectly acceptable to answer "[No] " provided a proper justification is given (e.g., "error bars are not reported because it would be too computationally expensive" or "we were unable to find the license for the dataset we used"). In general, answering "[No] " or "[NA] " is not grounds for rejection. While the questions are phrased in a binary way, we acknowledge that the true answer is often more nuanced, so please just use your best judgment and write a justification to elaborate. All supporting evidence can appear either in the main paper or the supplemental material, provided in appendix. If you answer [Yes] to a question, in the justification please point to the section(s) where related material for the question can be found.

IMPORTANT, please:

- **Delete this instruction block, but keep the section heading "NeurIPS Paper Checklist"**,
- **Keep the checklist subsection headings, questions/answers and guidelines below.**
- **Do not modify the questions and only use the provided macros for your answers**.

1. **Claims**

Question: Do the main claims made in the abstract and introduction accurately reflect the paper's contributions and scope?

Answer: [Yes]

Justification: The abstract includes the main contribution of the paper and to highlight it properly, there is a separate subsection in the Introduction that discusses on the main contribution of the paper

Guidelines:

- The answer NA means that the abstract and introduction do not include the claims made in the paper.
- The abstract and/or introduction should clearly state the claims made, including the contributions made in the paper and important assumptions and limitations. A No or NA answer to this question will not be perceived well by the reviewers.
- The claims made should match theoretical and experimental results, and reflect how much the results can be expected to generalize to other settings.
- It is fine to include aspirational goals as motivation as long as it is clear that these goals are not attained by the paper.

2. **Limitations**

Question: Does the paper discuss the limitations of the work performed by the authors?

Answer:[Yes]

Justification: We discuss the limitations of the paper in a separate section.

Guidelines:

- The answer NA means that the paper has no limitation while the answer No means that the paper has limitations, but those are not discussed in the paper.
- The authors are encouraged to create a separate "Limitations" section in their paper.
- The paper should point out any strong assumptions and how robust the results are to violations of these assumptions (e.g., independence assumptions, noiseless settings, model well-specification, asymptotic approximations only holding locally). The authors should reflect on how these assumptions might be violated in practice and what the implications would be.
- The authors should reflect on the scope of the claims made, e.g., if the approach was only tested on a few datasets or with a few runs. In general, empirical results often depend on implicit assumptions, which should be articulated.
- The authors should reflect on the factors that influence the performance of the approach. For example, a facial recognition algorithm may perform poorly when image resolution is low or images are taken in low lighting. Or a speech-to-text system might not be used reliably to provide closed captions for online lectures because it fails to handle technical jargon.
- The authors should discuss the computational efficiency of the proposed algorithms and how they scale with dataset size.
- If applicable, the authors should discuss possible limitations of their approach to address problems of privacy and fairness.
- While the authors might fear that complete honesty about limitations might be used by reviewers as grounds for rejection, a worse outcome might be that reviewers discover limitations that aren't acknowledged in the paper. The authors should use their best judgment and recognize that individual actions in favor of transparency play an important role in developing norms that preserve the integrity of the community. Reviewers will be specifically instructed to not penalize honesty concerning limitations.

3. **Theory assumptions and proofs**

Question: For each theoretical result, does the paper provide the full set of assumptions and a complete (and correct) proof?

Answer: [Yes]

Justification: The Methodology section contains detailed description of the proposed training strategy and the related algorithms. The supplementary material contains additional formulae and explanations.

Guidelines:

- The answer NA means that the paper does not include theoretical results.
- All the theorems, formulas, and proofs in the paper should be numbered and cross-referenced.
- All assumptions should be clearly stated or referenced in the statement of any theorems.
- The proofs can either appear in the main paper or the supplemental material, but if they appear in the supplemental material, the authors are encouraged to provide a short proof sketch to provide intuition.
- Inversely, any informal proof provided in the core of the paper should be complemented by formal proofs provided in appendix or supplemental material.
- Theorems and Lemmas that the proof relies upon should be properly referenced.

4. **Experimental result reproducibility**

Question: Does the paper fully disclose all the information needed to reproduce the main experimental results of the paper to the extent that it affects the main claims and/or conclusions of the paper (regardless of whether the code and data are provided or not)?

Answer: [Yes]

Justification: The Experiment section includes all the hyperparameter details and model variants. Further discussion on the choice of hyperparameter is included in the supplementary material.

Guidelines:

- The answer NA means that the paper does not include experiments.
- If the paper includes experiments, a No answer to this question will not be perceived well by the reviewers: Making the paper reproducible is important, regardless of whether the code and data are provided or not.
- If the contribution is a dataset and/or model, the authors should describe the steps taken to make their results reproducible or verifiable.
- Depending on the contribution, reproducibility can be accomplished in various ways. For example, if the contribution is a novel architecture, describing the architecture fully might suffice, or if the contribution is a specific model and empirical evaluation, it may be necessary to either make it possible for others to replicate the model with the same dataset, or provide access to the model. In general. releasing code and data is often one good way to accomplish this, but reproducibility can also be provided via detailed instructions for how to replicate the results, access to a hosted model (e.g., in the case of a large language model), releasing of a model checkpoint, or other means that are appropriate to the research performed.
- While NeurIPS does not require releasing code, the conference does require all submissions to provide some reasonable avenue for reproducibility, which may depend on the nature of the contribution. For example
  (a) If the contribution is primarily a new algorithm, the paper should make it clear how to reproduce that algorithm.
  (b) If the contribution is primarily a new model architecture, the paper should describe the architecture clearly and fully.
  (c) If the contribution is a new model (e.g., a large language model), then there should either be a way to access this model for reproducing the results or a way to reproduce the model (e.g., with an open-source dataset or instructions for how to construct the dataset).
  (d) We recognize that reproducibility may be tricky in some cases, in which case authors are welcome to describe the particular way they provide for reproducibility. In the case of closed-source models, it may be that access to the model is limited in some way (e.g., to registered users), but it should be possible for other researchers to have some path to reproducing or verifying the results.

5. **Open access to data and code**

   Question: Does the paper provide open access to the data and code, with sufficient instructions to faithfully reproduce the main experimental results, as described in supplemental material?

   Answer: [Yes]

   Justification: In the supplementary material we provide an anonymized GitHub repository of this paper.

   Guidelines:

   - The answer NA means that paper does not include experiments requiring code.
   - Please see the NeurIPS code and data submission guidelines (`https://nips.cc/public/guides/CodeSubmissionPolicy`) for more details.
   - While we encourage the release of code and data, we understand that this might not be possible, so "No" is an acceptable answer. Papers cannot be rejected simply for not including code, unless this is central to the contribution (e.g., for a new open-source benchmark).
   - The instructions should contain the exact command and environment needed to run to reproduce the results. See the NeurIPS code and data submission guidelines (`https://nips.cc/public/guides/CodeSubmissionPolicy`) for more details.
   - The authors should provide instructions on data access and preparation, including how to access the raw data, preprocessed data, intermediate data, and generated data, etc.
   - The authors should provide scripts to reproduce all experimental results for the new proposed method and baselines. If only a subset of experiments are reproducible, they should state which ones are omitted from the script and why.
   - At submission time, to preserve anonymity, the authors should release anonymized versions (if applicable).
   - Providing as much information as possible in supplemental material (appended to the paper) is recommended, but including URLs to data and code is permitted.

6. **Experimental setting/details**

   Question: Does the paper specify all the training and test details (e.g., data splits, hyperparameters, how they were chosen, type of optimizer, etc.) necessary to understand the results?

   Answer: [Yes]

   Justification: The Experiments section includes all the hyperparameter choice and the Methodology section includes the detailed description of the algorithm.

   Guidelines:

   - The answer NA means that the paper does not include experiments.
   - The experimental setting should be presented in the core of the paper to a level of detail that is necessary to appreciate the results and make sense of them.
   - The full details can be provided either with the code, in appendix, or as supplemental material.

7. **Experiment statistical significance**

   Question: Does the paper report error bars suitably and correctly defined or other appropriate information about the statistical significance of the experiments?

   Answer: [Yes]

   Justification: The Experiments section discusses the accuracy and performance of the models in detail.

   Guidelines:

   - The answer NA means that the paper does not include experiments.
   - The authors should answer "Yes" if the results are accompanied by error bars, confidence intervals, or statistical significance tests, at least for the experiments that support the main claims of the paper.

- The factors of variability that the error bars are capturing should be clearly stated (for example, train/test split, initialization, random drawing of some parameter, or overall run with given experimental conditions).
- The method for calculating the error bars should be explained (closed form formula, call to a library function, bootstrap, etc.)
- The assumptions made should be given (e.g., Normally distributed errors).
- It should be clear whether the error bar is the standard deviation or the standard error of the mean.
- It is OK to report 1-sigma error bars, but one should state it. The authors should preferably report a 2-sigma error bar than state that they have a 96% CI, if the hypothesis of Normality of errors is not verified.
- For asymmetric distributions, the authors should be careful not to show in tables or figures symmetric error bars that would yield results that are out of range (e.g. negative error rates).
- If error bars are reported in tables or plots, The authors should explain in the text how they were calculated and reference the corresponding figures or tables in the text.

8. **Experiments compute resources**

   Question: For each experiment, does the paper provide sufficient information on the computer resources (type of compute workers, memory, time of execution) needed to reproduce the experiments?

   Answer: [Yes]

   Justification: Details about the experimental resources are mentioned in the Supplementary material.

   Guidelines:

   - The answer NA means that the paper does not include experiments.
   - The paper should indicate the type of compute workers CPU or GPU, internal cluster, or cloud provider, including relevant memory and storage.
   - The paper should provide the amount of compute required for each of the individual experimental runs as well as estimate the total compute.
   - The paper should disclose whether the full research project required more compute than the experiments reported in the paper (e.g., preliminary or failed experiments that didn't make it into the paper).

9. **Code of ethics**

   Question: Does the research conducted in the paper conform, in every respect, with the NeurIPS Code of Ethics `https://neurips.cc/public/EthicsGuidelines`?

   Answer: [Yes]

   Justification: The NeurIPS Code of Ethics `https://neurips.cc/public/EthicsGuidelines` is followed while writing the paper.

   Guidelines:

   - The answer NA means that the authors have not reviewed the NeurIPS Code of Ethics.
   - If the authors answer No, they should explain the special circumstances that require a deviation from the Code of Ethics.
   - The authors should make sure to preserve anonymity (e.g., if there is a special consideration due to laws or regulations in their jurisdiction).

10. **Broader impacts**

    Question: Does the paper discuss both potential positive societal impacts and negative societal impacts of the work performed?

    Answer: [Yes]

    Justification: This paper fall under the category of optimizing neural networks.

    Guidelines:

    - The answer NA means that there is no societal impact of the work performed.

- If the authors answer NA or No, they should explain why their work has no societal impact or why the paper does not address societal impact.
- Examples of negative societal impacts include potential malicious or unintended uses (e.g., disinformation, generating fake profiles, surveillance), fairness considerations (e.g., deployment of technologies that could make decisions that unfairly impact specific groups), privacy considerations, and security considerations.
- The conference expects that many papers will be foundational research and not tied to particular applications, let alone deployments. However, if there is a direct path to any negative applications, the authors should point it out. For example, it is legitimate to point out that an improvement in the quality of generative models could be used to generate deepfakes for disinformation. On the other hand, it is not needed to point out that a generic algorithm for optimizing neural networks could enable people to train models that generate Deepfakes faster.
- The authors should consider possible harms that could arise when the technology is being used as intended and functioning correctly, harms that could arise when the technology is being used as intended but gives incorrect results, and harms following from (intentional or unintentional) misuse of the technology.
- If there are negative societal impacts, the authors could also discuss possible mitigation strategies (e.g., gated release of models, providing defenses in addition to attacks, mechanisms for monitoring misuse, mechanisms to monitor how a system learns from feedback over time, improving the efficiency and accessibility of ML).

11. **Safeguards**

    Question: Does the paper describe safeguards that have been put in place for responsible release of data or models that have a high risk for misuse (e.g., pretrained language models, image generators, or scraped datasets)?

    Answer: [NA]

    Justification: The data, models used in the paper are all publicly accessible.

    - The answer NA means that the paper poses no such risks.
    - Released models that have a high risk for misuse or dual-use should be released with necessary safeguards to allow for controlled use of the model, for example by requiring that users adhere to usage guidelines or restrictions to access the model or implementing safety filters.
    - Datasets that have been scraped from the Internet could pose safety risks. The authors should describe how they avoided releasing unsafe images.
    - We recognize that providing effective safeguards is challenging, and many papers do not require this, but we encourage authors to take this into account and make a best faith effort.

12. **Licenses for existing assets**

    Question: Are the creators or original owners of assets (e.g., code, data, models), used in the paper, properly credited and are the license and terms of use explicitly mentioned and properly respected?

    Answer: [Yes]

    Justification: All the existing work mentioned in the paper are properly cited.

    Guidelines:

    - The answer NA means that the paper does not use existing assets.
    - The authors should cite the original paper that produced the code package or dataset.
    - The authors should state which version of the asset is used and, if possible, include a URL.
    - The name of the license (e.g., CC-BY 4.0) should be included for each asset.
    - For scraped data from a particular source (e.g., website), the copyright and terms of service of that source should be provided.
    - If assets are released, the license, copyright information, and terms of use in the package should be provided. For popular datasets, `paperswithcode.com/datasets`

has curated licenses for some datasets. Their licensing guide can help determine the license of a dataset.
   - For existing datasets that are re-packaged, both the original license and the license of the derived asset (if it has changed) should be provided.
   - If this information is not available online, the authors are encouraged to reach out to the asset's creators.

13. **New assets**

    Question: Are new assets introduced in the paper well documented and is the documentation provided alongside the assets?

    Answer: [NA]

    Justification: [NA]

    Guidelines:

    - The answer NA means that the paper does not release new assets.
    - Researchers should communicate the details of the dataset/code/model as part of their submissions via structured templates. This includes details about training, license, limitations, etc.
    - The paper should discuss whether and how consent was obtained from people whose asset is used.
    - At submission time, remember to anonymize your assets (if applicable). You can either create an anonymized URL or include an anonymized zip file.

14. **Crowdsourcing and research with human subjects**

    Question: For crowdsourcing experiments and research with human subjects, does the paper include the full text of instructions given to participants and screenshots, if applicable, as well as details about compensation (if any)?

    Answer: [NA]

    Justification: [NA]

    Guidelines:

    - The answer NA means that the paper does not involve crowdsourcing nor research with human subjects.
    - Including this information in the supplemental material is fine, but if the main contribution of the paper involves human subjects, then as much detail as possible should be included in the main paper.
    - According to the NeurIPS Code of Ethics, workers involved in data collection, curation, or other labor should be paid at least the minimum wage in the country of the data collector.

15. **Institutional review board (IRB) approvals or equivalent for research with human subjects**

    Question: Does the paper describe potential risks incurred by study participants, whether such risks were disclosed to the subjects, and whether Institutional Review Board (IRB) approvals (or an equivalent approval/review based on the requirements of your country or institution) were obtained?

    Answer: [NA]

    Justification: [NA]

    Guidelines:

    - The answer NA means that the paper does not involve crowdsourcing nor research with human subjects.
    - Depending on the country in which research is conducted, IRB approval (or equivalent) may be required for any human subjects research. If you obtained IRB approval, you should clearly state this in the paper.
    - We recognize that the procedures for this may vary significantly between institutions and locations, and we expect authors to adhere to the NeurIPS Code of Ethics and the guidelines for their institution.

- For initial submissions, do not include any information that would break anonymity (if applicable), such as the institution conducting the review.

16. **Declaration of LLM usage**

    Question: Does the paper describe the usage of LLMs if it is an important, original, or non-standard component of the core methods in this research? Note that if the LLM is used only for writing, editing, or formatting purposes and does not impact the core methodology, scientific rigorousness, or originality of the research, declaration is not required.

    Answer: [NA] .

    Justification: LLMS are not used for any important component of the paper.

    Guidelines:

    - The answer NA means that the core method development in this research does not involve LLMs as any important, original, or non-standard components.
    - Please refer to our LLM policy (`https://neurips.cc/Conferences/2025/LLM`) for what should or should not be described.